Computer Assisted Mechanics and Engineering Sciences, 4: 645–666, 1997.

Equilibrium method for postprocessing and error estimation in the finite element method

Erwin Stein and Stephan Ohnimus
Institute for Structural and Numerical Mechanics, University of Hannover
Appelstraße 9A, D-30167 Hannover, Germany
e-mail: stein@leibniz.ibnm.uni-hannover.de

(Received December 20, 1996)

Modeling of elastic thin-walled beams, plates and shells as 1D and 2D boundary value problems is valid in undisturbed subdomains. Disturbances near supports and free edges, in the vicinity of concentrated loads and at thickness jumps cannot be described by 1D and 2D BVP's. In these disturbed subdomains dimensional (d)-adaptivity and possibly model (m)-adaptivity have to be performed and coupled with mixed h- and/or p-adaptivity by hierarchically expanded test spaces in order to guarantee a reliable and efficient overall solution. Using residual error estimators coupled with anisotropic error estimation and mesh refinement, an efficient adaptive calculation is possible. This residual estimator is based on stress jumps along the internal boundaries and residua of the field equation in L_2 norms. In this paper, we introduce an equilibrium method for calculation of the internal tractions on local patches using orthogonality conditions. These tractions are equilibrated with respect to the global equilibrium condition of forces and bending moments. We derive a new error estimation based on jumps between the new tractions and the tractions calculated with the stresses of the current finite element solution solution. This posterior equilibrium method (PEM) is based on the local calculation of improved stress tractions along the internal boundaries of element patches with continuity condition in normal directions. The introduction of new tractions is a method which can be regarded as a stepwise hybrid displacement method or as Trefftz method for a Neumann problem of element patches. An additional and important advantage is the local numerical solution and the model error estimation based on the equilibrated tractions.

1. Introduction

The deformations and stresses of elastic beams, plates in bending and shells, modeled approximately by 1D and 2D theories via kinematic hypotheses, show considerable deviations from the solutions of 3D theory in disturbed subdomains, like boundary layers, haunched thicknesses or concentrated loads. It is possible to establish a coupled adaptive process by hierarchical projections from a rather general theory, e.g. of 3D elasticity, see [5, 9] and such to improve not only the numerical solution of an approximated theory by hp-adaptivity and d-adaptivity (d=dimension), e.g. by higher shear elastic deformation modes instead of the Kirchhoff–Love or Reissner–Mindlin hypotheses, but also the mathematical model in disturbed subdomains by m-adaptivity (m=model), e.g. extension to complete 3D elasticity or elastoplasticity. Such one can start with simple 2D elastic theories of plates and shells, e.g. with Kirchhoff–Love hypothesis, and proceed to the complete Lame equations (expansion method) or, in a reverse procedure (reduction method), [10, 20, 17, 21, 19]. These new strategies yield a quality jump of FEM regarding real engineering problems.

A new idea for error estimation is to formulate a local boundary value problem based on improved stress calculation. It is possible to compute C^0 continuous stresses in the whole system with an a posteriori so-called equilibrium method, see [6, 16, 15]. It is also possible to get better stress fields with solving a subproblem on a patch, see [1]. With these better local element boundary tractions it is possible to formulate a local variational problem for estimating the model-error with respect to an hierarchically expanded model, e.g. elasto-plasticity with hardening. This is a main topic of our current research.

2. Organization of integrated *HPDM*-adaptive processes

Adaptivity is organized threefold, see Fig. 1. We start with a 3D master model of highest admitted complexity, e.g. 3D linear elasticity or elasto-plasticity with hardening and define the hierarchical submodels and their test spaces.

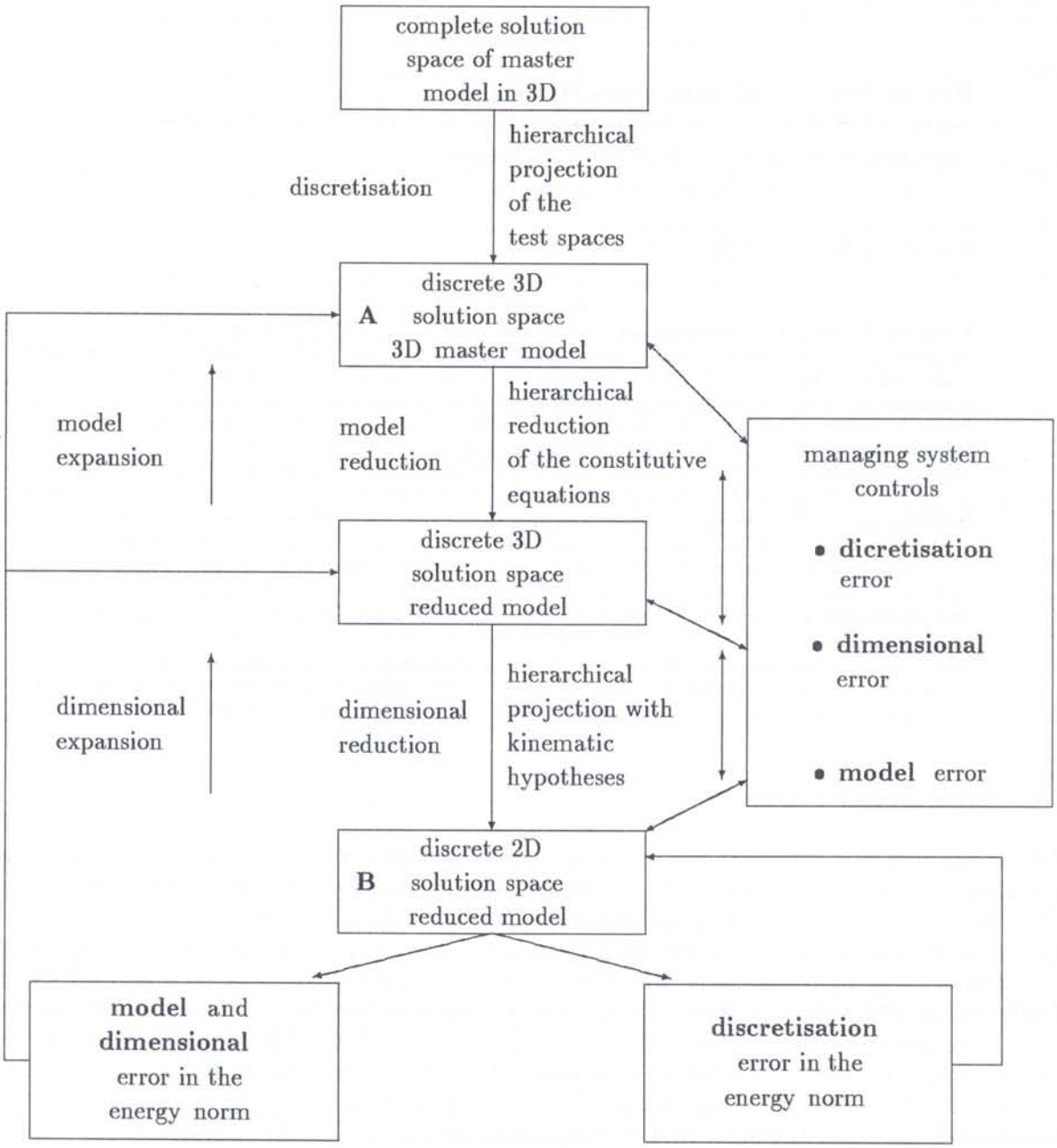

Fig. 1. Scheme of the complete *hpdm*-adaptive process; starting with A: Reduction method; starting with B: Expansion method

The first task is the projection from the complete solution and test space onto the discrete approximation and test space. The second task is the definition of a nested sequence of *simplified models* called *model reductions*. Its error analysis is the basis for model adaptivity (*m-adaptivity*).

Then we project the discrete *solution space* of the reduced model (e.g. reduced shear force integration with plane stress condition) onto a reduced space (e.g. with Mindlin hypothesis), named

dimensional reduction. For the *a posteriori* error analysis of the corresponding discretized problem we get dimensional adaptivity (*d-adaptivity*) as an *expansion strategy*, controlled by comparisons between polynomial expansion (d_p-adaptivity) or mesh refining (d_h-adaptivity), especially in thickness direction. By checking the *discretization error in the current approximation space* of a specific model we get the well-known *h-* or *p-adaptivity* for the solution.

Thus, there are three nested classes of errors, *the discretization, the dimensional and the model error.* For model adaptivity it is not useful to check the model error alone (without dimensional expansion), because coupling influences can lead to locking effects and inconsistencies.

If we want to check the model-error we must testwise enhance the approximation space at the same time. Such we get two different types of residua, see also [19]. It is evident that expansion strategies correspond to engineering thinking and working, namely to proceed from lower to higher complexity, especially for large and complicated structures. Additionally this method yields less computational effort than the reduction method for stiffened thin-walled structures.

3. Classification of error estimators for solution and models within elliptic boundary value problems

In this section a classification of different error estimators is given.

(A) Algebraic including error estimation for dimension and model adaptivity, (e.g.: Hackbusch 1989, [7, 8]).
Problems are:

(1) Global solution and model error estimation is necessary;

(2) Special solution techniques are necessary for defect correction.

(B) *Residual error estimation on patches* for solution and dimension adaptivity (e.g.: Babuška, Rheinboldt 1978, [3, 4]; Johnson, Hansbo 1992, [10]; Stein, Ohnimus 1992, e.g. [20, 19]).

Solution and model error estimation, including robust and effective calculation of model residuals is known for hierarchical reduction techniques applied to plates in bending without haunches, [5, 14]. In case of expansion method, residual errors are not useful for model adaptivity because of strong locking effects for plates and shells.

(C) Error estimation by *Posterior Equilibrium Method (PEM) on patches* for solution, dimension and model adaptivity (e.g.: Bufler, Stein 1970 [6], Stein, Ahmad 1973,1977, e.g. [16], Stein [15], Ladevèze, Leguillon 1983 [11], Ladevèze, Maunder 1996, [12]; Ainsworth, Oden 1992 [1], Oden, Wu, Ainsworth 1994 [13]).

Problems are that the mathematical analysis is still in progress and the choice of adequate norms for local error estimation needs further research.

(D) *L_2-Projection* of σ_h (smoothing), Zienkiewicz, Zhu 1987, [23], and *Superconvergent Patch Recovery* (SPR)-techniques [24, 25].

Problems are that *hp*-adaptivity is hard to realize, the regularity of the solution has to be known and that it does not seem to be applicable for model adaptivity.

In the next sections we explain the basic idea of the algebraic defect correction method (A), the analysis for the anisotropic residual error estimation on patches for solution and dimension adaptivity (B) and the new error estimation by posterior equilibrium method (PEM) on patches for solution, dimension and model adaptivity (C).

4. Algebraic defect correction method including error estimation

From the engineering point of view the primar calculation starts with a reduced model in a reduced dimension. After FE-discretisation of the displacements we get linear algebraic system of equations

$$\mathbf{K}_h \hat{\mathbf{u}}_h = \hat{\mathbf{p}}_h\,, \qquad \mathbf{u}_h \in \mathbf{V}_h \subset \mathbf{V}\,. \tag{1}$$

The discretization and the dimensional error $\mathbf{e}$ of the displacements is defined with respect to an expanded approximation space as well as in the enlarged dimension.

$$\mathbf{e} = \mathbf{e}_h + \mathbf{e}_+, \qquad \mathbf{e} \in \mathbf{V}, \qquad \mathbf{e}_h \in \mathbf{V}_h, \qquad \mathbf{e}_+ \in \mathbf{V} \ominus \mathbf{V}_h\,. \tag{2}$$

For the *model adaptivity* we introduce a *correction-stiffness matrix* $\Delta\mathbf{K}_h$

$$\tilde{\mathbf{K}}_h = \mathbf{K}_h + \Delta\mathbf{K} \quad \text{with} \quad \|\Delta\mathbf{K}_h\|_E < \|\tilde{\mathbf{K}}_h\|_E\,. \tag{3}$$

$\tilde{\mathbf{K}}_h$ is the enhanced stiffness matrix including the model correction with respect to the expanded model in subdomains. For hierarchically expanded test spaces the error estimation yields

$$\begin{pmatrix} \mathbf{K}_h + \Delta\mathbf{K}_h & \mathbf{L}_+ \\ \mathbf{L}_+^{\mathrm{T}} & \mathbf{H}_+ \end{pmatrix} \begin{pmatrix} \hat{\mathbf{u}}_h + \hat{\mathbf{e}}_h \\ \hat{\mathbf{e}}_+ \end{pmatrix} = \begin{pmatrix} \hat{\mathbf{p}}_h \\ \hat{\mathbf{p}}_+ \end{pmatrix}, \tag{4}$$

where $\mathbf{L}_+$ is the coupling matrix between the approximation space $\mathbf{V}_h$ and the higher order approximation space $\mathbf{V}_+$.

$$\begin{pmatrix} \mathbf{K}_h + \Delta\mathbf{K}_h & \mathbf{L}_+ \\ \mathbf{L}_+^{\mathrm{T}} & \mathbf{H}_+ \end{pmatrix} \begin{pmatrix} \hat{\mathbf{e}}_h \\ \hat{\mathbf{e}}_+ \end{pmatrix} = \begin{pmatrix} -\Delta\mathbf{K}\hat{\mathbf{u}}_h \\ \hat{\mathbf{p}}_+ - \mathbf{L}_+^{\mathrm{T}}\hat{\mathbf{u}}_h \end{pmatrix}. \tag{5}$$

The *model error* is associated with the residual $-\Delta\mathbf{K}\hat{\mathbf{u}}_h$, and the *discretisation* and the *dimensional* errors are associated with the residuals $\hat{\mathbf{p}}_+ - \mathbf{L}_+^{\mathrm{T}}\hat{\mathbf{u}}_h$.

Equation (5) represents a global problem, and the task is to find effective algorithms to use the information of the undisturbed system for the computation of the defect correction due to model adaptivity in the subdomains. Further information and ideas to this problem are given by Hackbusch [7, 8].

5. Anisotropic residual error estimation for second order elliptic problems

The anisotropic residual error estimation is based on two main strategies. The first is the calculation of the stress jumps (or jumps of traction) $\mathbf{J}$ inside the domain, the traction jumps $\mathbf{J}$ along the natural system boundaries and controlling of the equilibrium equation ($\operatorname{div}\boldsymbol{\sigma} + \mathbf{f} = \mathbf{R}$) within the elements Ω_i. The second idea is to check these residuals ($\mathbf{J}$ and $\mathbf{R}$) in a useful norm, e.g. the energy norm. For the calculation of the error in the energy norm. We show that the residuals have to be projected onto the higher order test spaces.

5.1. Galerkin orthogonality and solution spaces

With the basic results from Babuška and Miller [4], Babuška and Schwab [5] and Johnson [10] the fundamentals of residual error analysis are available. These results are extended to the analysis of anisotropic error estimators on patches, depending on refinement directions, polynomial expansions and on the dimension of the test functions. We start with the geometrically linear equations in

vector-analytical notation $\boldsymbol{\varepsilon} := \frac{1}{2}\left[\operatorname{grad}\mathbf{u} + \operatorname{grad}\mathbf{u}^{\mathrm{T}}\right]$ and the linear equilibrium conditions in 3D linear elasticity

$$\operatorname{div}\boldsymbol{\sigma}(\mathbf{u}) + \mathbf{f} = \mathbf{0}, \qquad \mathbf{u} = \mathbf{u}(\mathbf{x}), \qquad \forall \mathbf{x} \in \Omega \subset \mathbf{R}^3, \tag{6}$$

Hooke's generalized elasticity law

$$\boldsymbol{\sigma}(\mathbf{u}) = \lambda \operatorname{div}\mathbf{u}\,\mathbf{I} + 2\mu\boldsymbol{\varepsilon}(\mathbf{u}), \tag{7}$$

and mixed boundary conditions

$$\mathbf{u} = \mathbf{0} \quad \text{on } \Gamma_u \qquad \text{and} \qquad \boldsymbol{\sigma}\mathbf{n} = \bar{\mathbf{t}} \quad \text{on } \Gamma_t; \qquad \Gamma_u \cap \Gamma_t = \{\}. \tag{8}$$

$\mathbf{u}(\mathbf{x})$ is the displacement vector in a cartesian frame, $\boldsymbol{\varepsilon}(\mathbf{u})$ is the linear strain tensor with $\boldsymbol{\varepsilon} := \frac{1}{2}(u_{i,j} + u_{j,i})\ \mathbf{e}_i \otimes \mathbf{e}_j$; $\boldsymbol{\sigma}$ is the stress tensor with $\boldsymbol{\sigma} = \sigma_{ij}\mathbf{e}_i \otimes \mathbf{e}_j$ and μ, λ are the Lamé coefficients with $\lambda = \dfrac{E\nu}{(1+\nu)(1-2\nu)}$ and $\mu = \dfrac{E}{2(1+\nu)}$. The weak form of equilibrium is

$$\int_\Omega (\operatorname{div}\boldsymbol{\sigma} + \mathbf{f})\,\mathbf{v}\,\mathrm{d}V = 0 \quad \text{for } \mathbf{u} \in \mathbf{V}, \qquad \forall \mathbf{v} \in \mathbf{V} \tag{9}$$

with the space $\mathbf{V}$ of test functions $\mathbf{v}(\mathbf{x})$

$$\mathbf{V} = \left\{ \mathbf{v} \in \left[H_0^1(\Omega)\right]^3 : \mathbf{v} = \mathbf{0} \quad \text{on } \Gamma_u \right\}, \tag{10}$$

where $\mathbf{v}$ is a test function of the test space $\mathbf{V}$. Integrating Eq. (9) by parts, yields the variational form

$$g(\mathbf{u}, \mathbf{v}) = \int_{\Gamma_t} \boldsymbol{\sigma}\mathbf{n}\mathbf{v}\,\mathrm{d}O - \int_\Omega \boldsymbol{\sigma}\operatorname{grad}\mathbf{v}\,\mathrm{d}V + \int_\Omega \mathbf{f}\mathbf{v}\,\mathrm{d}V = 0, \qquad \partial\Omega = \Gamma_t \cup \Gamma_u \tag{11}$$

and further

$$g(\mathbf{u}, \mathbf{v}) = \int_{\Gamma_t} \bar{\mathbf{t}}\mathbf{v}\,\mathrm{d}O - \int_\Omega \boldsymbol{\sigma}(\mathbf{u})\,\boldsymbol{\varepsilon}(\mathbf{v})\,\mathrm{d}V + \int_\Omega \mathbf{f}\mathbf{v}\,\mathrm{d}V = 0 \tag{12}$$

$$\rightarrow \int_\Omega \boldsymbol{\sigma}(\mathbf{u})\,\boldsymbol{\varepsilon}(\mathbf{v})\,\mathrm{d}V = \int_{\Gamma_t} \bar{\mathbf{t}}\mathbf{v}\,\mathrm{d}O + \int_\Omega \mathbf{f}\mathbf{v}\,\mathrm{d}V \tag{13}$$

condensed as

$$a(\mathbf{u}, \mathbf{v}) = L(\mathbf{v}) \qquad \forall \mathbf{v} \in \mathbf{V} \tag{14}$$

with the bilinear form

$$a(\mathbf{u}, \mathbf{v}) = \int_\Omega \boldsymbol{\sigma}(\mathbf{u})\,\boldsymbol{\varepsilon}(\mathbf{v})\,\mathrm{d}V \tag{15}$$

and the linear form

$$L(\mathbf{v}) = \int_{\Gamma_t} \bar{\mathbf{t}}\mathbf{v}\,\mathrm{d}O + \int_\Omega \mathbf{f}\mathbf{v}\,\mathrm{d}V. \tag{16}$$

The energy norm of the approximated displacement $\mathbf{u}$ reads

$$\|\mathbf{u}\|_{E(\Omega)} = \sqrt{a(\mathbf{u}, \mathbf{u})}. \tag{17}$$

With the Finite Element Method we introduce an hierarchical projection from the complete solution space onto a discrete approximation space with the same boundary conditions. The restricted solution space $\mathbf{V} \rightarrow \mathbf{V}_h$, i.e. $\mathbf{v} \rightarrow \mathbf{v}_h$ and $\mathbf{u} \rightarrow \mathbf{u}_h$ is the approximation space with $\mathbf{v}_h, \mathbf{u}_h \in \mathbf{V}_h \subset \mathbf{V}$ defined as

$$\mathbf{V}_h = \left\{ \mathbf{v}_h, \mathbf{v} \in \left[H_0^1(\Omega)\right]^3 \right\} : \ \mathbf{v} = 0 \quad \text{on } \Gamma_u \quad \text{and} \quad \mathbf{v}_h = \boldsymbol{\pi}_h\mathbf{v}, \tag{18}$$

where $\boldsymbol{\pi}_h$ is a hierarchical projection operator which projects the complete test space onto the current approximation space. The FE solution space $\mathbf{V}_h$ is fully embedded in $\mathbf{V}$.

5.2. A posteriori error analysis

The main issue is the determination of the error with respect to sequential higher orders of approximation spaces on local subdomains (patches). The error estimation with respect to the complete solution space is not effective, and it is not possible.

Starting with the variational form, see Eq. (14), the FE approximation reads

$$a(\mathbf{u}_h, \mathbf{v}_h) = L(\mathbf{v}_h); \quad \forall \mathbf{v}_h \in \mathbf{V}_h; \quad \mathbf{u}_h \in \mathbf{V}_h. \tag{19}$$

With the split of the displacement error $\mathbf{e}$ into two parts

$$\mathbf{e} := \mathbf{u} - \mathbf{u}_h = \mathbf{e}_h + \mathbf{e}_+; \quad \mathbf{e} \in \mathbf{V}; \quad \mathbf{e}_+ \in \mathbf{V}_+ = \mathbf{V} \ominus \mathbf{V}_h \tag{20}$$

and a corresponding split of the test functions $\mathbf{v} \in \mathbf{V}$ into $\mathbf{v}_h$ and the enhanced term $\mathbf{v}_+ \in \mathbf{V}_+ = \mathbf{V} \ominus \mathbf{V}_h$

$$\mathbf{v} = \mathbf{v}_h + \mathbf{v}_+ = \boldsymbol{\pi}_h \mathbf{v} + \boldsymbol{\pi}_+ \mathbf{v} \tag{21}$$

with the hierarchical projection operators

$$\boldsymbol{\pi}_h : \mathbf{v}_h = \boldsymbol{\pi}_h \mathbf{v}, \quad \mathbf{v}_h \in \mathbf{V}_h, \mathbf{v} \in \mathbf{V}, \tag{22}$$

$$\boldsymbol{\pi}_+ : \mathbf{v}_+ = \boldsymbol{\pi}_+ \mathbf{v}, \quad \mathbf{v}_+ \in \mathbf{V} \ominus \mathbf{V}_h, \mathbf{v} \in \mathbf{V}, \tag{23}$$

we get the orthogonality of the error $\mathbf{e}$ with respect to the test functions $\mathbf{v}_h$ in the energy norm

$$a(\mathbf{e}, \mathbf{v}_h) = a(\mathbf{u}, \mathbf{v}_h) - a(\mathbf{u}_h, \mathbf{v}_h), \tag{24}$$

$$a(\mathbf{e}, \mathbf{v}_h) = L(\mathbf{v}_h) - L(\mathbf{v}_h) = 0, \quad \forall \mathbf{v}_h \in \mathbf{V}_h. \tag{25}$$

With these results, the weak form is given by the current solution $\mathbf{u}_h \in \mathbf{V}_h$, by the displacement error $\mathbf{e} \in \mathbf{V}$ and by the hierarchically projected higher order test functions $\boldsymbol{\pi}_+ \mathbf{v} \in \mathbf{V} \ominus \mathbf{V}_h$. Starting from Eq. (14) this results in

$$\underbrace{a(\mathbf{u}_h, \boldsymbol{\pi}_h \mathbf{v})}_{L(\mathbf{v}_h)} + a(\mathbf{u}_h, \boldsymbol{\pi}_+ \mathbf{v}) + a(\mathbf{e}, \mathbf{v}) = L(\mathbf{v}_h) + L(\boldsymbol{\pi}_+ \mathbf{v}) \tag{26}$$

and finally in the main equation of local residual error analysis, by using Eq. (25), see also [4,10,19],

$$a(\mathbf{e}, \mathbf{v}) = a(\mathbf{e}, \boldsymbol{\pi}_+ \mathbf{v}) = L(\boldsymbol{\pi}_+ \mathbf{v}) - a(\boldsymbol{\pi}_h \mathbf{u}, \boldsymbol{\pi}_+ \mathbf{v}); \quad \forall \mathbf{v} \in \mathbf{V}; \quad \mathbf{u}, \mathbf{e} \in \mathbf{V}. \tag{27}$$

The error η in the energy norm is

$$\eta^2 = ||\mathbf{e}||^2_{E(\Omega)} = a(\mathbf{e}, \mathbf{e}) = L(\boldsymbol{\pi}_+ \mathbf{e}) - a(\mathbf{u}_h, \boldsymbol{\pi}_+ \mathbf{e}), \tag{28}$$

and the relative error in the energy norm reads

$$\eta_r^2 = \frac{a(\mathbf{e}, \mathbf{e})}{a(\mathbf{u}, \mathbf{u})} = \frac{\|\mathbf{e}\|^2_{E(\Omega)}}{\|\mathbf{u}\|^2_{E(\Omega)}}. \tag{29}$$

In case of robust problems, only two additional hierarchical test and trial functions for each coordinate direction, i.e. $p_+ = 1; 2$ or $h_+ = \frac{h}{2}, \frac{h}{4}$ are necessary, see [18].

5.3. Residual formulation of the local element error

Starting from the main equation of error analysis, Eq. (27), the whole domain is divided into local FE subdomains Ω_e; $\bigcup_{e=1}^{n_e} \Omega_e = \tilde{\Omega}$ $\left(\tilde{\Omega} \simeq \Omega\right)$. This yields after partial integration

$$a(\mathbf{e},\boldsymbol{\pi}_+\mathbf{v}) = \bigcup_{e=1}^{n_e} \left\{ \int_{\Gamma_{t_e}} \bar{\mathbf{t}}\,(\boldsymbol{\pi}_+\mathbf{v})\ \mathrm{d}O + \int_{\Omega_e} \mathbf{f}\,(\boldsymbol{\pi}_+\mathbf{v})\ \mathrm{d}V \right.$$
$$\left. - \int_{\partial\Omega_e} \boldsymbol{\sigma}\,(\mathbf{u}_h)\,\mathbf{n}\,(\boldsymbol{\pi}_+\mathbf{v})\ \mathrm{d}O + \int_{\Omega_e} \operatorname{div}\boldsymbol{\sigma}\,(\mathbf{u}_h)\,(\boldsymbol{\pi}_+\mathbf{v})\ \mathrm{d}V \right\}, \tag{30}$$

where $\partial\Omega_e = \Gamma_{t_e} \cup \Gamma_{u_e} \cup \Gamma_{i_e}$, Γ_{i_e} are the interior element boundaries of the domain Ω, and further we get

$$a(\mathbf{e},\boldsymbol{\pi}_+\mathbf{v}) = \bigcup_{e=1}^{n_e} \left\{ \int_{\Omega_e} (\mathbf{f} + \operatorname{div}\boldsymbol{\sigma}\,(\mathbf{u}_h))\,(\boldsymbol{\pi}_+\mathbf{v})\ \mathrm{d}V \right.$$
$$\left. + \int_{\Gamma_{t_e}} [\bar{\mathbf{t}} - \boldsymbol{\sigma}\,(\mathbf{u}_h)\,\mathbf{n}]\,(\boldsymbol{\pi}_+\mathbf{v})\ \mathrm{d}O - \int_{\Gamma_{i_e}} [\boldsymbol{\sigma}\,(\mathbf{u}_h)\,\mathbf{n}]\,(\boldsymbol{\pi}_+\mathbf{v})\ \mathrm{d}O \right\}, \tag{31}$$

with the residua

$$\mathbf{R} := \mathbf{f} + \operatorname{div}\boldsymbol{\sigma}\,(\mathbf{u}_h) \quad \text{in } \Omega_e; \qquad \mathbf{J} := \bar{\mathbf{t}} - \boldsymbol{\sigma}\,(\mathbf{u}_h)\,\mathbf{n} \quad \text{on } \Gamma_{t_e} \tag{32}$$

and the jumps of projected stresses at interelement boundaries

$$\mathbf{J} := \underbrace{\boldsymbol{\sigma}\,(\mathbf{u}_h)\,\mathbf{n}^+|_{\Gamma_i^+}}_{\mathbf{t}^+} + \underbrace{\boldsymbol{\sigma}\,(\mathbf{u}_h)\,\mathbf{n}^-|_{\Gamma_i^-}}_{\mathbf{t}^-} \qquad \text{on } \Gamma_i\,. \tag{33}$$

Finally we arrive at the variational form described by the residua of the approximated solution $\mathbf{u}_h$

$$a(\mathbf{e},\boldsymbol{\pi}_+\mathbf{v}) = \bigcup_{e=1}^{n_e} \left\{ \int_{\Omega_e} \mathbf{R}\,(\boldsymbol{\pi}_+\mathbf{v})\ \mathrm{d}V + \int_{\Gamma_{t_e}} \mathbf{J}_b\,(\boldsymbol{\pi}_+\mathbf{v})\ \mathrm{d}O - \frac{1}{2}\int_{\Gamma_{i_e}} \mathbf{J}\,(\boldsymbol{\pi}_+\mathbf{v})\ \mathrm{d}O \right\},$$
$$\forall \mathbf{v} \in \mathbf{V}; \mathbf{e} \in \mathbf{V}\,. \tag{34}$$

By setting $\mathbf{v} = \mathbf{e}$ we get the error in the energy norm $\|\mathbf{e}\|_{E(\Omega)}$

$$\|\mathbf{e}\|^2_{E(\Omega)} = a(\mathbf{e},\mathbf{e}) = \bigcup_{e=1}^{n_e} \left\{ \int_{\Omega_e} \mathbf{R}\,(\boldsymbol{\pi}_+\mathbf{e})\ \mathrm{d}V + \int_{\Gamma_{t_e}} \mathbf{J}_b\,(\boldsymbol{\pi}_+\mathbf{e})\ \mathrm{d}O - \frac{1}{2}\int_{\Gamma_{i_e}} \mathbf{J}\,(\boldsymbol{\pi}_+\mathbf{e})\ \mathrm{d}O \right\}. \tag{35}$$

5.4. Residual error projection from a patch onto a unit patch

The goal is the computation of absolute error estimatorsn realized on element patches. The main technical idea is the introduction of a bijective invariant energy transformation. The domain Ω_e of the current element is extended onto the patch $\mathcal{P}_e$ with 8 elements in 2D problems and 26 elements in 3D problems. The residuum $\mathbf{R}$ is defined in Ω_e and $\mathbf{J}$ on $\partial\Omega_e$. The error $\mathbf{e}$ is defined on $\mathcal{P}_e$ with setting $\mathbf{e} = \mathbf{0}$ on the outer boundary $\Gamma_{\mathcal{P}_e}$, i.e. Dirichlet boundary conditions for $\mathcal{P}_e$, see Fig. 2. Now this fixed patch $\mathcal{P}_e$ is mapped onto the parameter space and yields the domain $\mathcal{I}$ with the fixed boundary $\Gamma_{\mathcal{I}}$. The shape functions are expanded from the parametric element domain $i \subset \mathcal{I}$ to patch $\mathcal{I}$ regarding the fixed boundary. The stiffness matrix $\tilde{\mathbf{K}}$ of this *patch* $\mathcal{I}$ can be easily computed from such of the interior element domain i by multiplication of the coefficients with factors 1, 2, 4 or 8, see Table 1. $\tilde{\mathbf{K}}$ is symmetric and positive definite.

Table 1. Factors for the coefficients of the local 3D stiffness matrix for element $i \subset \mathcal{I}$ in the unit path $\mathcal{I}$

factor	associated coefficient
1	inside domain i
2	on a surface of domain i
4	at an edge of the domain i
8	in a corner of the domain i

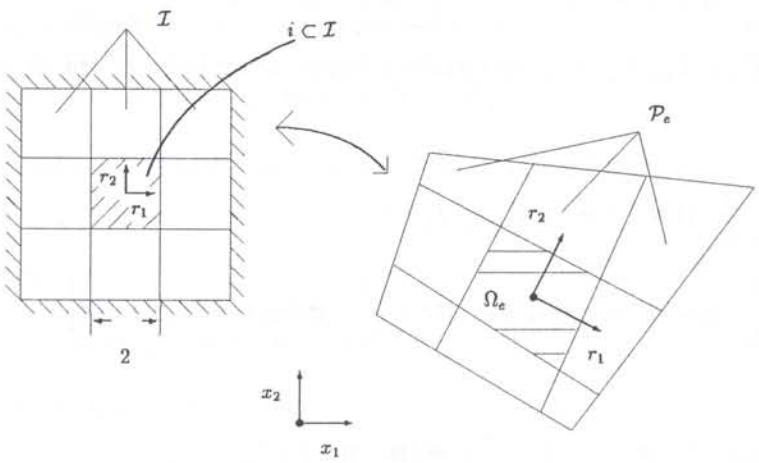

Fig. 2. Isoparametric transformation from a patch $\mathcal{P}_e$ surrounding Ω_e into the parametric patch $\mathcal{I}$ with Dirichlet boundary conditions, surrounding the parameter element $i \subset \mathcal{I}$

Another simplified error estimation consists in restricting the bilinear form to the higher order approximation space only. This modification of the locally transformed stiffness matrix for element i yields a regular and positive definite stiffness matrix, associated with a domain witout boundary conditions. The regularity of $\tilde{\mathbf{K}}$ results from the fact that the higher terms of the approximation space don't include rigid body modes. For the linear form $a(\mathbf{e}, \mathbf{v})$ we get with Eq. (25)

$$a(\mathbf{e}, \mathbf{u}) = a(\mathbf{e}, \boldsymbol{\pi}_+ \mathbf{v}) \approx a(\boldsymbol{\pi}_+ \mathbf{e}, \boldsymbol{\pi}_+ \mathbf{v}) \qquad \forall \mathbf{v} \in \mathbf{V}. \tag{36}$$

Equation (27), applied to the patch $\mathcal{P}_e$, yields

$$a(\mathbf{e}, \boldsymbol{\pi}_+ \mathbf{v})_{\mathcal{P}_e} = L(\boldsymbol{\pi}_+ \mathbf{v}) - a(\mathbf{u}_h, \boldsymbol{\pi}_+ \mathbf{v})_{\mathcal{P}_e}; \qquad \forall \mathbf{v} \in \mathbf{V} \tag{37}$$

and

$$\int_{\mathcal{P}_e} \nabla_x(\mathbf{e})\, \mathbf{C} \nabla_x(\mathbf{v})\, \mathrm{d}V = \int_{\Omega_e} \mathbf{R} \boldsymbol{\pi}_+ \mathbf{v}\, \mathrm{d}V + \int_{\partial \Omega_e} \mathbf{J} \boldsymbol{\pi}_+ \mathbf{v}\, \mathrm{d}O. \tag{38}$$

The bijective transformation of Ω_e onto the corresponding cube element $i \subset \mathcal{I}$ needs the Jacobian matrix $\boldsymbol{\mathcal{J}}$

$$\boldsymbol{\mathcal{J}} := [\mathcal{J}_{ij}] = \left[\frac{\partial x_i}{\partial r_j}\right] = \nabla_r \mathbf{x} \tag{39}$$

with the following property for a vector-valued differentiable function $\mathbf{f}(\mathbf{x})$ with approximately constant Jacobian matrix $\boldsymbol{\mathcal{J}}$ within Ω_e

$$\nabla_x \mathbf{f}(\mathbf{x}) = \nabla_x \boldsymbol{\mathcal{J}} \tilde{\mathbf{f}}(\mathbf{r}) = \nabla_x \nabla_r \mathbf{x} \tilde{\mathbf{f}}(\mathbf{r}) = \nabla_r \tilde{\mathbf{f}}(\mathbf{r}) \cdot \underbrace{\mathbf{I}}_{\nabla_x \mathbf{x}}. \tag{40}$$

Such the bijective transformations of the error $\mathbf{e}$ and the test function $\mathbf{v}$ from $\mathcal{P}_e$ to the energy invariant error $\tilde{\mathbf{e}}$ in $\mathcal{I}$ are

$$\mathbf{e} = \boldsymbol{\mathcal{J}}\tilde{\mathbf{e}}; \qquad \mathbf{v} = \boldsymbol{\mathcal{J}}\tilde{\mathbf{v}} \quad \text{with} \quad \tilde{\mathbf{e}}, \tilde{\mathbf{v}} \in \mathbf{V}_{\mathcal{P}_e}. \tag{41}$$

Inserting the mapped fields into Eq. (37) results in

$$\int_{\mathcal{P}_e} \nabla_x(\boldsymbol{\mathcal{J}}\tilde{\mathbf{e}}) \cdot \mathbf{C} \cdot \nabla_x(\boldsymbol{\mathcal{J}}\tilde{\mathbf{v}})\, \mathrm{d}V = \int_{\Omega_e} \mathbf{R} \cdot \boldsymbol{\pi}_+ \boldsymbol{\mathcal{J}}\tilde{\mathbf{v}}\, \mathrm{d}V + \int_{\partial\Omega_e} \mathbf{J} \cdot \boldsymbol{\pi}_+ \boldsymbol{\mathcal{J}}\tilde{\mathbf{v}}\, \mathrm{d}O \tag{42}$$

and is transformed into

$$\max(\det \boldsymbol{\mathcal{J}}_{\Omega_e}) \cdot \int_{\mathcal{I}} \nabla_r(\tilde{\mathbf{e}}) \cdot \mathbf{C} \cdot \nabla_r(\tilde{\mathbf{v}})\, \mathrm{d}V = \int_{\mathcal{I}} \tilde{\mathbf{R}} \cdot \boldsymbol{\pi}_+ \tilde{\mathbf{v}}\, \mathrm{d}V + \int_{\partial\mathcal{I}} \tilde{\mathbf{J}} \cdot \boldsymbol{\pi}_+ \tilde{\mathbf{v}}\, \mathrm{d}O \tag{43}$$

with the bijective transformation of the residua

$$\tilde{\mathbf{R}} = \mathbf{R} \cdot \boldsymbol{\mathcal{J}} \cdot \det(\boldsymbol{\mathcal{J}})_{\Omega_e}, \quad \tilde{\mathbf{J}} = \mathbf{J} \cdot \boldsymbol{\mathcal{J}} \cdot \det(\boldsymbol{\mathcal{J}})_{\partial\Omega_e}. \tag{44}$$

For an upper bound of the error estimation we have to set

$$\max(\det \boldsymbol{\mathcal{J}}_{\Omega_e}) = \max_{\mathbf{x}\in\Omega_e}(\det \boldsymbol{\mathcal{J}}(\mathbf{x})), \tag{45}$$

such that an energy-invariant formulation of the weak form for the unit patch $\mathcal{I}$ is achieved by

$$\begin{aligned} a(\mathbf{e}, \mathbf{v})_{\mathcal{P}_e} &= a(\mathbf{e}, \boldsymbol{\pi}_+\mathbf{v})_{\mathcal{P}_e} \leq \max(\det \boldsymbol{\mathcal{J}}_{\Omega_e}) \cdot a(\tilde{\mathbf{e}}, \boldsymbol{\pi}_+\tilde{\mathbf{v}})_{\mathcal{I}} \\ &\leq \int_{\mathcal{I}} \tilde{\mathbf{R}} \cdot \boldsymbol{\pi}_+ \tilde{\mathbf{v}}\, \mathrm{d}V + \int_{\partial\mathcal{I}} \tilde{\mathbf{J}} \cdot \boldsymbol{\pi}_+ \tilde{\mathbf{v}}\, \mathrm{d}O \qquad \forall \tilde{\mathbf{v}} \in \mathbf{V} \quad \text{and} \quad \tilde{\mathbf{e}} \in \mathbf{V}. \end{aligned} \tag{46}$$

5.5. Residual error estimation

From the weak form of the unit patch, Eq. (46), the bilinar form is written in matrix notation as

$$a(\tilde{\mathbf{e}}, \boldsymbol{\pi}_+\tilde{\mathbf{v}})_{\mathcal{I}} = a(\tilde{\mathbf{e}}, \tilde{\mathbf{v}})_{\mathcal{I}} = \hat{\tilde{\mathbf{e}}}^{\mathrm{T}} \tilde{\mathbf{K}} \hat{\tilde{\mathbf{v}}}, \tag{47}$$

with the interpolations and the stiffness matrix

$$\tilde{\mathbf{e}} = \mathbf{N}\hat{\tilde{\mathbf{e}}}, \quad \tilde{\mathbf{v}} = \mathbf{N}\hat{\tilde{\mathbf{v}}} \quad \text{and} \quad \tilde{\mathbf{K}} = \int_{\mathcal{I}} \tilde{\mathbf{B}}^{\mathrm{T}} \mathbf{C} \tilde{\mathbf{B}}\, \mathrm{d}V, \tag{48}$$

where $\mathbf{N}(\mathbf{r})$ is the matrix of shape functions in the coordinates of the parameter space. The first terms of the linear form reads

$$\int_{\mathcal{I}} \tilde{\mathbf{R}} \cdot \boldsymbol{\pi}_+ \mathbf{v}\, \mathrm{d}V = \hat{\tilde{\mathbf{R}}} \tilde{\mathbf{L}}_R \hat{\tilde{\mathbf{v}}}, \tag{49}$$

with

$$\tilde{\mathbf{R}} = \mathbf{N}\hat{\tilde{\mathbf{R}}} \quad \text{and} \quad \tilde{\mathbf{L}}_R = \int_{\mathcal{I}} \mathbf{N}\mathbf{N}_+\, \mathrm{d}V, \tag{50}$$

where $\mathbf{N}_+$ is the matrix of hierarchically expanded shape functions. The transformed stress jumps on $\partial\mathcal{I}$ yield the second term of the linear form

$$\int_{\partial\mathcal{I}} \tilde{\mathbf{J}} \cdot \boldsymbol{\pi}_+ \tilde{\mathbf{v}}\, \mathrm{d}O = \hat{\tilde{\mathbf{J}}}^{\mathrm{T}} \tilde{\mathbf{L}}_J \hat{\tilde{\mathbf{v}}}, \tag{51}$$

with

$$\tilde{\mathbf{J}} = \mathbf{N}\hat{\tilde{\mathbf{J}}} \quad \text{and} \quad \tilde{\mathbf{L}}_J = \int_{\partial\mathcal{I}} \mathbf{N}\mathbf{N}_+\, \mathrm{d}O. \tag{52}$$

Note that overroofed letters denote nodal values at finite element nodes. Thus, inserting Eqs. (47)–(52) into Eq. (46), we get the main equation of error analysis, computed on a unit patch as

$$\max(\det \mathcal{J}_{\Omega_e}) \cdot \hat{\tilde{\mathbf{e}}}^{\mathrm{T}} \tilde{\mathbf{K}} \hat{\tilde{\mathbf{v}}} = \hat{\tilde{\mathbf{R}}}^{\mathrm{T}} \tilde{\mathbf{L}}_R \hat{\tilde{\mathbf{v}}} + \hat{\tilde{\mathbf{J}}}^{\mathrm{T}} \tilde{\mathbf{L}}_J \hat{\tilde{\mathbf{v}}}. \tag{53}$$

The corresponding energy norm of the error η_e is

$$\eta_e^2 = \max(\det \mathcal{J}_{\Omega_e})\, \hat{\tilde{\mathbf{e}}}^{\mathrm{T}} \tilde{\mathbf{K}} \hat{\tilde{\mathbf{e}}} = \hat{\tilde{\mathbf{R}}}^{\mathrm{T}} \tilde{\mathbf{L}}_R \hat{\tilde{\mathbf{e}}} + \hat{\tilde{\mathbf{J}}}^{\mathrm{T}} \tilde{\mathbf{L}}_J \hat{\tilde{\mathbf{e}}}. \tag{54}$$

Herewith it is possible to derive two different error estimators, the first oriented to *Johnson's and Hansbo's* [10] proposal using an eigenvalue problem, and the second one proposed here, using the inversion of $\mathbf{K}$.

5.6. Error estimation with a general eigenvalue problem

At first, two base vector systems $\hat{\tilde{\mathbf{g}}}_{R_i}$ and $\hat{\tilde{\mathbf{g}}}_{J_i}$ are defined which are orthonormal with respect to the energy norm on patch $\mathcal{I}$, i.e.

$$\hat{\tilde{\mathbf{g}}}_{R_i}{}^{\mathrm{T}} \tilde{\mathbf{K}} \hat{\tilde{\mathbf{g}}}_{R_i} = \delta_{ij}\,, \qquad \hat{\tilde{\mathbf{g}}}_{J_i}{}^{\mathrm{T}} \tilde{\mathbf{K}} \hat{\tilde{\mathbf{g}}}_{J_i} = \delta_{ij} \tag{55}$$

with the conditions for general eigenvalue problems, see Eqs. (49) and (51)

$$\begin{aligned} &\hat{\tilde{\mathbf{g}}}_{R_i}{}^{\mathrm{T}} \tilde{\mathbf{L}}_R \hat{\tilde{\mathbf{g}}}_{R_i} - c_{R_i}^2 \hat{\tilde{\mathbf{g}}}_{R_i}{}^{\mathrm{T}} \tilde{\mathbf{K}} \hat{\tilde{\mathbf{g}}}_{R_i} = 0\,, \\ &\hat{\tilde{\mathbf{g}}}_{J_i}{}^{\mathrm{T}} \tilde{\mathbf{L}}_J \hat{\tilde{\mathbf{g}}}_{J_i} - c_{R_i}^2 \hat{\tilde{\mathbf{g}}}_{J_i}{}^{\mathrm{T}} \tilde{\mathbf{K}} \hat{\tilde{\mathbf{g}}}_{J_i} = 0\,. \end{aligned} \tag{56}$$

The displacement error, Eq. (48), can be represented by these base vectors $\hat{\tilde{\mathbf{g}}}_{R_i}$ and $\hat{\tilde{\mathbf{g}}}_{J_i}$ as

$$\hat{\tilde{\mathbf{e}}} = \sum_i \tilde{e}_{R_i} \cdot \hat{\tilde{\mathbf{g}}}_{R_i} \quad \text{with} \quad \tilde{e}_{R_i} = \hat{\tilde{\mathbf{e}}}^{\mathrm{T}} \tilde{\mathbf{K}} \hat{\tilde{\mathbf{g}}}_{R_i} \tag{57}$$

and

$$\hat{\tilde{\mathbf{e}}} = \sum_i \tilde{e}_{J_i} \cdot \hat{\tilde{\mathbf{g}}}_{J_i} \quad \text{with} \quad \tilde{e}_{J_i} = \hat{\tilde{\mathbf{e}}}^{\mathrm{T}} \tilde{\mathbf{K}} \hat{\tilde{\mathbf{g}}}_{J_i}, \tag{58}$$

with the coefficients $\tilde{e}_{R_i}$ and $\tilde{e}_{J_i}$. Then we get the bilinear form for the unit patch element $\mathcal{I}$ in the parameter space form Eq. (54)

$$\max(\det \mathcal{J}_{\Omega_e}) \cdot \hat{\tilde{\mathbf{e}}}^{\mathrm{T}} \tilde{\mathbf{K}} \hat{\tilde{\mathbf{e}}} = \sum_{ij} \tilde{e}_{R_i} \cdot \hat{\tilde{\mathbf{g}}}_{R_i}{}^{\mathrm{T}} \tilde{\mathbf{K}} \hat{\tilde{\mathbf{g}}}_{Rj} \cdot \tilde{e}_{Rj} = \sum_i \tilde{e}_{R_i}^2 = \sum_{ij} \tilde{e}_{J_i} \cdot \hat{\tilde{\mathbf{g}}}_{J_i}{}^{\mathrm{T}} \tilde{\mathbf{K}} \hat{\tilde{\mathbf{g}}}_{Jj} \cdot \tilde{e}_{Jj}\,. \tag{59}$$

The error norm η in the form of Eq. (54) results in

$$\eta^2 = \max(\det \mathcal{J}_{\Omega_e}) \cdot \hat{\tilde{\mathbf{e}}}^{\mathrm{T}} \tilde{\mathbf{K}} \hat{\tilde{\mathbf{e}}} = \sum_i \hat{\tilde{\mathbf{R}}}^{\mathrm{T}} \tilde{\mathbf{L}}_R \cdot \underbrace{\hat{\tilde{\mathbf{g}}}_{R_i} \cdot \tilde{e}_{R_i}}_{\hat{\tilde{\mathbf{e}}}} + \sum_i \hat{\tilde{\mathbf{J}}}^{\mathrm{T}} \tilde{\mathbf{L}}_J \cdot \underbrace{\hat{\tilde{\mathbf{g}}}_{Ji} \cdot \tilde{e}_{Ji}}_{\hat{\tilde{\mathbf{e}}}}\,. \tag{60}$$

With the triangle inequality we get the estimation

$$\max(\det \mathcal{J}_{\Omega_e}) \cdot \hat{\tilde{\mathbf{e}}}^{\mathrm{T}} \tilde{\mathbf{K}} \hat{\tilde{\mathbf{e}}} \leq \left\{ \sum_i \left[\hat{\tilde{\mathbf{R}}}^{\mathrm{T}} \tilde{\mathbf{L}}_R \hat{\tilde{\mathbf{g}}}_{R_i} \right]^2 \cdot \underbrace{\sum_i [\tilde{e}_{Ri}]^2}_{a(\tilde{\mathbf{e}},\tilde{\mathbf{e}})_{\mathcal{I}}} + \sum_i \left[\hat{\tilde{\mathbf{J}}}^{\mathrm{T}} \tilde{\mathbf{L}}_J \hat{\tilde{\mathbf{g}}}_{Ji} \right]^2 \cdot \underbrace{\sum_i [\tilde{e}_{Ri}]^2}_{a(\tilde{\mathbf{e}},\tilde{\mathbf{e}})_{\mathcal{I}}} \right\}^{1/2}, \tag{61}$$

and finally, the improved error estimator computed in the parameter space reads

$$\begin{aligned} \eta^2 = a(\mathbf{e},\mathbf{e})_{\mathcal{P}_e} &\leq \max(\det \mathcal{J}_{\Omega_e}) \cdot a(\tilde{\mathbf{e}},\tilde{\mathbf{e}})_{\mathcal{I}} \\ &\leq \left\{ \sum_i \left[\hat{\tilde{\mathbf{R}}}^{\mathrm{T}} \tilde{\mathbf{L}}_R \hat{\tilde{\mathbf{g}}}_{R_i} \right]^2 + \sum_i \left[\hat{\tilde{\mathbf{J}}}^{\mathrm{T}} \tilde{\mathbf{L}}_J \hat{\tilde{\mathbf{g}}}_{Ji} \right]^2 \right\} \cdot \min(\det \mathcal{J}_{\Omega_e})^{-1}\,. \end{aligned} \tag{62}$$

$\hat{\tilde{\mathbf{R}}}$ and $\hat{\tilde{\mathbf{J}}}$ are transformed nodal residua from the real patch $\mathcal{P}_e$ onto the unit patch $\mathcal{I}$.

Note: For an upper bound estimation it is necessary to define the factor $\det \boldsymbol{\mathcal{J}}_\Omega$ as minimum, because of the division of this term in Eq. (62).

$$\min(\det \boldsymbol{\mathcal{J}}_{\Omega_e}) = \min_{\mathbf{x}\in\boldsymbol{\Omega}_e}(\det \boldsymbol{\mathcal{J}}(\mathbf{x})). \tag{63}$$

5.7. Error estimation by inversion of the local stiffness matrix for the unit patch

Starting from Eq. (53), the solution exists for every $\hat{\tilde{\mathbf{v}}}$ if

$$\max(\det \boldsymbol{\mathcal{J}}_{\Omega_e}) \cdot \tilde{\mathbf{K}}\hat{\tilde{\mathbf{e}}} = \tilde{\mathbf{L}}_R^{\mathrm{T}}\hat{\tilde{\mathbf{R}}} + \tilde{\mathbf{L}}_J^{\mathrm{T}}\hat{\tilde{\mathbf{J}}} \tag{64}$$

holds. $\tilde{\mathbf{K}}$ is a positive definite matrix (see Table 1) and can be inverted as

$$\hat{\tilde{\mathbf{e}}} = \min(\det \boldsymbol{\mathcal{J}}_{\Omega_e}) \cdot \tilde{\mathbf{K}}^{-1} \cdot \left\{ \tilde{\mathbf{L}}_R^{\mathrm{T}}\hat{\tilde{\mathbf{R}}} + \tilde{\mathbf{L}}_J^{\mathrm{T}}\hat{\tilde{\mathbf{J}}} \right\}. \tag{65}$$

We set $\det \boldsymbol{\mathcal{J}}_\Omega = \min(\det \boldsymbol{\mathcal{J}}_{\Omega_e})$ in order to get an upper bound. Such the error η in the energy norm finally results in

$$\begin{aligned} \eta_e^2 &= a(\mathbf{e},\mathbf{e})_{\mathcal{P}_e} \le \max(\det \boldsymbol{\mathcal{J}}_{\Omega_e}) \cdot a(\tilde{\mathbf{e}},\tilde{\mathbf{e}})_{\mathcal{I}} \\ &\le \left\{ \hat{\tilde{\mathbf{R}}}^{\mathrm{T}} \tilde{\mathbf{L}}_R + \hat{\tilde{\mathbf{J}}}\tilde{\mathbf{L}}_J \right\} \tilde{\mathbf{K}}^{-1} \left\{ \tilde{\mathbf{L}}_R^{\mathrm{T}}\hat{\tilde{\mathbf{R}}} + \tilde{\mathbf{L}}_J^{\mathrm{T}}\hat{\tilde{\mathbf{J}}} \right\} \min(\det \boldsymbol{\mathcal{J}}_{\Omega_e})^{-1}. \end{aligned} \tag{66}$$

These estimators Eq. (62) and Eq. (66) look similar. The computation effort is nearly the same. Note that the calculation has only to be performed once. The eigenvalue method admits a fast approximated estimation of dominating terms whereas the inversion method is a strict upper bound estimation.

5.8. Anisotropic residuum based error indicators

A classical result of the error analysis for linear elastic problem, see e.g. *Babuška and Miller* [2] or *Johnston and Hansbo* [10], is the following estimation

$$\eta_{enh}^2 = a(\mathbf{e},\mathbf{e}) = \|\mathbf{e}\|_{E(\Omega_e)}^2 = \|\mathbf{u}-\mathbf{u}_h\|_{E(\Omega_e)}^2 \le \|c_R h \mathbf{R}\|_{L_2(\Omega_e)}^2 + \left\| \tfrac{1}{2} c_J h^{1/2} \mathbf{J} \right\|_{L_2(\partial\Omega_e)}^2 \tag{67}$$

with the residual of the interior domain, $\mathbf{R} = \mathbf{f} + \operatorname{div} \boldsymbol{\sigma}_h(\mathbf{u}_h)$ and the projected stress jumps at the boundaries, $\mathbf{J}$. But the L_2- norms in the formulas above have averaging and smoothing properties, especially for elements with large length to width ratios (anisotropic elements). A suitable error estimator starts with the equation

$$\eta_e^2 = a(\mathbf{e},\mathbf{e}) = a(\mathbf{e},\mathbf{e}_+) = \int_{\Omega_e} \mathbf{R}\cdot\mathbf{e}_+ \mathrm{d}\mathbf{x} + \frac{1}{2}\int_{\partial\Omega_e} \mathbf{J}\cdot\mathbf{e}_+ \mathrm{d}s \tag{68}$$

with the unknown updated error $\mathbf{e}_+ \in \mathbf{V}_+ := \mathbf{V} \ominus \mathbf{V}_h$ of the displacements. The strategy is now to choose the next higher possible degree of polynomials in the approximation space or a suitable refinement for every direction $z \in r,s,t$ of the parameter coordinates. The approximation space is adjusted to the anisotropic refinement (directions of the anisotropic coordinates r,s,t) with $N_+^z(r,s,t)$ denoting the refined shape functions

$$\mathbf{e}_+^z = N_+^z(r,s,t)\cdot\hat{\mathbf{e}}_+^z \in \mathbf{V}_+ \subset \mathbf{V}; z = r,s,t \quad \text{and} \quad \mathbf{e}^z = N^z(r,s,t)\cdot\hat{\mathbf{e}}^z \in \mathbf{V}. \tag{69}$$

This yields an approximated error, which is asum of the error components in the directions r, s, t

$$\eta_z^2 = \sum_e \left\{ \int_{\Omega_e} \mathbf{R} \cdot \mathbf{e}_+^z \mathrm{d}\mathbf{x} + \frac{1}{2} \int_{\partial\Omega_e} \mathbf{J} \cdot \mathbf{e}_+^z \mathrm{d}s \right\} \quad \text{and} \quad \eta^2 = \sum_{z=r,s,t} \eta_z^2. \tag{70}$$

In total local estimators are avalaible on a unit patch which test the three directions and, e.g., $p_+ = 1; 2$ or $h_+ = \frac{h}{2}; \frac{h}{4}$. These general results are mapped in an energy-invariant way to the real patches in order to control h- and p-adaptivity.

5.9. Example of a plate stiffened by a floor beam

This example was investigated in [22] by using different combinations of plate–beam and folded plate theories without adaptivity. The system data are shown in Fig. 3a.

The selfadaptive process with convergence to the elastic 3D solution is shown in Figs. 3b and 3c–d displaying the relative error in the energy norm, the effectivity index and the convergence rate of the energy. The calculation with only 2D degenerated plate elements does not converge to the correct solution. The full 3D h-adaptive method with triquadratic elements converges to the 3D solution but not as efficiently as the h–d-adaptive process. Figure 4a shows the stresses τ_{xz} of the 2D reduced model after 13th step of the 2D h-adaptive process, and Fig. 4b shows the realistic stresses τ_{xz} of the full 3D model after 13th step of the 2D to 3D h–d-adaptive process, especially in disturbed subdomains.

6. Posterior Equilibrium Method (PEM) for error estimation on patches

The posterior equilibrium method is based on the local calculation of improved stress tractions along the internal boundaries with continuity condition in normal directions. This introduction of new tractions is a method which can be explained as a stepwise hybrid displacement method or as a Trefftz method for Neumann problems on element patches, see also [6, 16, 12]. We formulate regularized varational problems on patches which equilibrate these new tractions with the known nodal forces form the previous finite element solution, using additional regularizations. With these new equilibrated tractions it is possible to introduce a new error estimator for the discretization error and also especially for the model error. The unknown locally equilibrated boundary tractions $\mathbf{t}_h$ on patches k have to fulfil the weak equilibrium conditions

$$\int_{\partial\Omega_k} \mathbf{t}_h^{\mathrm{T}} \mathbf{v}_h \mathrm{d}O = \hat{\bar{\mathbf{p}}}_h^{\mathrm{T}}(\mathbf{u}_h) \hat{\mathbf{v}}_h \qquad \forall \mathbf{v}_h \in \mathbf{V}\,;\ \mathbf{t}_h \in \mathbf{L}_2 \tag{71}$$

with the previous algebraic equation system for $\mathbf{u}_h$, yielding the element nodal forces

$$\hat{\bar{\mathbf{p}}}_h(\mathbf{u}_h) = \mathbf{K}_e \hat{\mathbf{u}}_h \tag{72}$$

and the test and functions (virtual displacements)

$$\mathbf{v}_h = \mathbf{N}_v \hat{\mathbf{v}}_h. \tag{73}$$

The unknown local locally equilibrated boundary tractions are parametrized as

$$\mathbf{t}_h = \bar{\mathbf{N}}_t \hat{\bar{\mathbf{t}}}_h \tag{74}$$

from Eqs. (71)–(74) we get

$$\hat{\bar{\mathbf{t}}}_h \cdot \underbrace{\int_{\partial\Omega} \bar{\mathbf{N}}_t^{\mathrm{T}} \mathbf{N}_v \mathrm{d}O}_{\mathbf{S}} \cdot \hat{\mathbf{v}}_h = \hat{\bar{\mathbf{p}}}_h^{\mathrm{T}}(\mathbf{u}_h) \hat{\mathbf{v}}_h \qquad \forall \hat{\mathbf{v}}_h \in \hat{\mathbf{V}}_h\,, \tag{75}$$

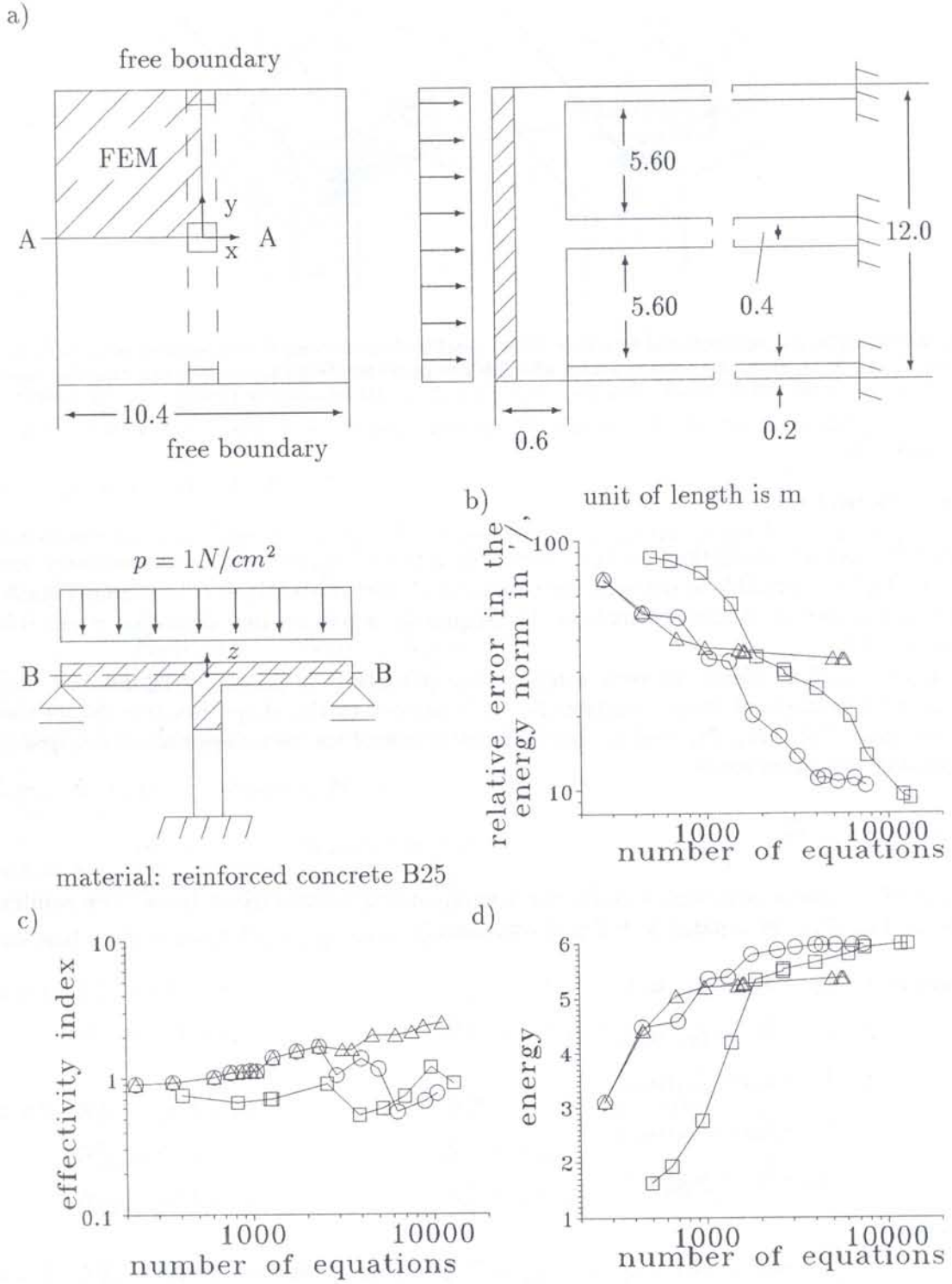

Fig. 3. Example of a plate stiffened by a floor beam; Description: △: h-adaptivity, 2D model; □: h-adaptivity, 3D model; ◯: h- d-adaptivity, 2D to 3D model; system data: E=30000 MPa, ν=0.2; a) system; b) relative error in the energy norm in %; c) effectivity index of the estimated error with respect to the error in the energy norm for $N \approx 20000$ (N=number of equations); d) convergence rate in $10^2 J$ (quarter of the system);

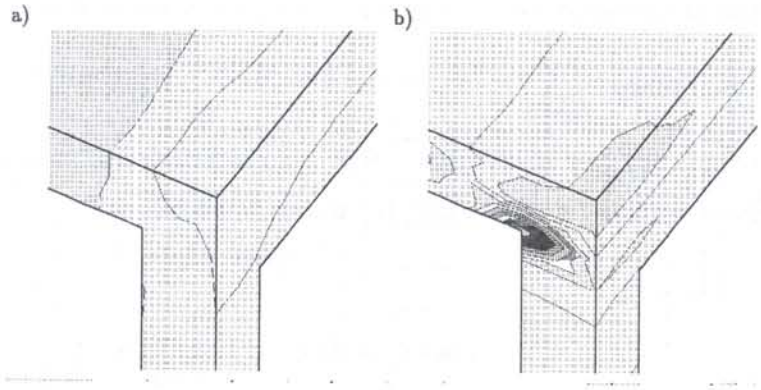

Fig. 4. Example of a plate stiffened by a floor beam; quarter of the system; a) transverse shear stresses τ_{xz} in section A–A, Fig. 3, of the 2D reduced model after 13th steps of the 2D h-adaptive process, near the column; b) stresses τ_{xz} of the full 3D model after 13th step of the 2D to 3D hd-adaptive process, near the column.

which results in

$$\mathbf{S}^{\mathrm{T}}\hat{\hat{\mathbf{t}}}_h = \hat{\hat{\mathbf{p}}}_h(\mathbf{u}_h). \tag{76}$$

Only C^0 continuity conditions for $\mathbf{t}_h$ in normal direction of element surfaces is necessary, and due to $\mathbf{t}_h \in \mathbf{L}_2(\Omega_k)$ it is possible to describe the equilibrated tractions without C^0 continuity conditions in tangential direction of element surfaces. Consequently, a patch-wise calculation is possible, see Ainsworth (1992) [1].

To avoid coupling effects between neighbouring patches it is necessary to describe the new tractions with orthogonal shape function $\bar{\mathbf{N}}_t$ with respect to the shape function $\mathbf{N}_v$ of the test space, see Eqs. (75), (76), $\mathbf{N}_v$ and $\bar{\mathbf{N}}_t$ are different bases of the same approximation space. The orthogonality condition reads

$$\int_{\partial\Omega} \bar{N}_t^i N_{vj} \mathrm{d}O = \delta_j^i, \tag{77}$$

such that $\mathbf{N}_v$ forms a covariant and $\bar{\mathbf{N}}_t$ the corresponding contravariant basis. The equilibrium conditions, Eq. (75), for a patch k in Fig. 5 are given by

$$\begin{aligned}
\text{Element 1:}\quad & \hat{\hat{t}}_{h1} - \hat{\hat{t}}_{h5} = \hat{\hat{p}}_{h1}(\mathbf{u}_h)\,, \\
2:\quad & \hat{\hat{t}}_{h2} - \hat{\hat{t}}_{h1} = \hat{\hat{p}}_{h2}(\mathbf{u}_h)\,, \\
3:\quad & \hat{\hat{t}}_{h3} - \hat{\hat{t}}_{h2} = \hat{\hat{p}}_{h3}(\mathbf{u}_h)\,, \\
4:\quad & \hat{\hat{t}}_{h4} - \hat{\hat{t}}_{h3} = \hat{\hat{p}}_{h4}(\mathbf{u}_h)\,, \\
5:\quad & \hat{\hat{t}}_{h5} - \hat{\hat{t}}_{h4} = \hat{\hat{p}}_{h5}(\mathbf{u}_h)
\end{aligned} \tag{78}$$

and result in

$$\overbrace{\begin{bmatrix} +1 & & & & -1 \\ -1 & +1 & & & \\ & -1 & +1 & & \\ & & -1 & +1 & \\ & & & -1 & +1 \end{bmatrix}}^{\mathbf{T}} \cdot \overbrace{\begin{bmatrix} \hat{\hat{t}}_{h1} \\ \hat{\hat{t}}_{h2} \\ \hat{\hat{t}}_{h3} \\ \hat{\hat{t}}_{h4} \\ \hat{\hat{t}}_{h5} \end{bmatrix}}^{\hat{\hat{\mathbf{t}}}_h} = \overbrace{\begin{bmatrix} \hat{\hat{p}}_{h1}(\mathbf{u}_h) \\ \hat{\hat{p}}_{h2}(\mathbf{u}_h) \\ \hat{\hat{p}}_{h3}(\mathbf{u}_h) \\ \hat{\hat{p}}_{h4}(\mathbf{u}_h) \\ \hat{\hat{p}}_{h5}(\mathbf{u}_h) \end{bmatrix}}^{\hat{\hat{\mathbf{p}}}_h(\mathbf{u}_h)}, \tag{79}$$

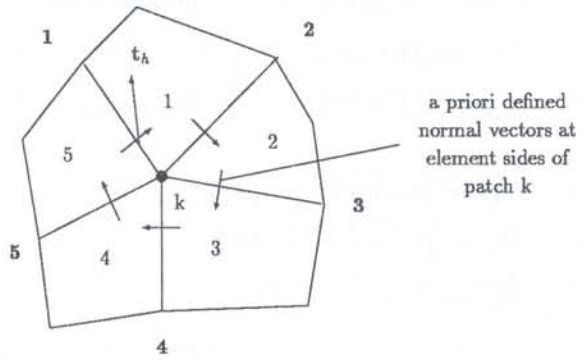

Fig. 5. Patch k for node k; element boundaries are described by side numbers $i = 1, 5$. A priori defined normal vectors at element sides i are plotted.

where $\mathbf{T}$ can be interpretated as a topology matrix. Equation (79) can be condensed as

$$\mathbf{T}\cdot\hat{\bar{\mathbf{t}}}_h = \hat{\bar{\mathbf{p}}}_h(\mathbf{u}_h)\ ; \quad \det(\mathbf{T}^{\mathrm{T}}\mathbf{T}) = \mathbf{0}. \tag{80}$$

We introduce covariant Lagrangean base functions and their contravariant base functions

$$\mathbf{N}_v(r,s) = \mathbf{N}_{\mathcal{L}}(r,s) = \mathbf{N}_{\mathcal{L}}(r) \otimes \mathbf{N}_{\mathcal{L}}(s)\,, \tag{81}$$

$$\bar{\mathbf{N}}_t(r,s) = \frac{\bar{\mathbf{N}}_{\mathcal{L}}(r,s)}{\det(\boldsymbol{\mathcal{J}}(r,s))_{\partial\Omega_e}} = \frac{\bar{\mathbf{N}}_{\mathcal{L}}(r) \otimes \bar{\mathbf{N}}_{\mathcal{L}}(s)}{\det(\boldsymbol{\mathcal{J}}(r,s))_{\partial\Omega_e}}\,, \tag{82}$$

or the hierarchical Legendre base functions, respectively

$$\mathbf{N}_v(r,s) = \mathbf{N}_{\mathcal{H}}(r,s) = \mathbf{N}_{\mathcal{H}}(r) \otimes \mathbf{N}_{\mathcal{H}}(s)\,, \tag{83}$$

$$\bar{\mathbf{N}}_t(r,s) = \frac{\bar{\mathbf{N}}_{\mathcal{H}}(r,s)}{\det(\boldsymbol{\mathcal{J}}(r,s))_{\partial\Omega_e}} = \frac{\bar{\mathbf{N}}_{\mathcal{H}}(r) \otimes \bar{\mathbf{N}}_{\mathcal{H}}(s)}{\det(\boldsymbol{\mathcal{J}}(r,s))_{\partial\Omega_e}}\,. \tag{84}$$

The co- and contravariant Lagrange base functions for $p = 1, 2, 3$ are

$$\begin{aligned}
p=1 \quad & N^1_{\mathcal{L}0} = \tfrac{1}{2}(1-r) && \bar{N}^{10}_{\mathcal{L}} = \tfrac{1}{2}(1-3r) \\
& N^1_{\mathcal{L}1} = \tfrac{1}{2}(1+r) && \bar{N}^{11}_{\mathcal{L}} = \tfrac{1}{2}(1+3r) \\
p=2 \quad & N^2_{\mathcal{L}0} = \tfrac{1}{2}r(1-r) && \bar{N}^{20}_{\mathcal{L}} = \tfrac{3}{8}(-2-4r+10r^2) \\
& N^2_{\mathcal{L}1} = 1-r^2 && \bar{N}^{21}_{\mathcal{L}} = \tfrac{3}{8}(3-5r^2) \\
& N^2_{\mathcal{L}2} = \tfrac{1}{2}r(1+r) && \bar{N}^{22}_{\mathcal{L}} = \tfrac{3}{8}(-2+4r+10r^2) \\
p=3 \quad & N^3_{\mathcal{L}0} = \tfrac{1}{16}(-1+r+9r^2-9r^3) && \bar{N}^{30}_{\mathcal{L}} = \tfrac{1}{4}(-3+15r+15r^2-35r^3) \\
& N^3_{\mathcal{L}1} = \tfrac{1}{16}(9-27r-9r^2+27r^3) && \bar{N}^{31}_{\mathcal{L}} = \tfrac{1}{108}(99-285r-135r^2+385r^3) \\
& N^3_{\mathcal{L}2} = \tfrac{1}{16}(9+27r-9r^2-27r^3) && \bar{N}^{32}_{\mathcal{L}} = \tfrac{1}{108}(99+285r-135r^2-385r^3) \\
& N^3_{\mathcal{L}3} = \tfrac{1}{16}(-1-r+9r^2+9r^3) && \bar{N}^{33}_{\mathcal{L}} = \tfrac{1}{4}(-3-15r+15r^2+35r^3),
\end{aligned} \tag{85}$$

with

$$\delta^j_i = \int_{-1}^{+1} N^p_{\mathcal{L}_i}(r) \cdot \bar{N}^{pj}_{\mathcal{L}}(r)\mathrm{d}r. \tag{86}$$

The co- and contravariant hierarchical Legendre base functions for $p = 1, 2, 3$ are

$$
\begin{aligned}
p=1 \quad & N^1_{\mathcal{H}0} = \tfrac{1}{2}(1-r) \quad && \bar{N}^{10}_{\mathcal{H}} = \tfrac{1}{2}(1-3r) \\
& N^1_{\mathcal{H}1} = \tfrac{1}{2}(1+r) && \bar{N}^{11}_{\mathcal{H}} = \tfrac{1}{2}(1+3r) \\
p=2 \quad & N^2_{\mathcal{H}0} = \tfrac{1}{2}(1-r) && \bar{N}^{20}_{\mathcal{H}} = \tfrac{1}{4}(-3-6r+15r^2) \\
& N^2_{\mathcal{H}1} = \tfrac{1}{2}(1+r) && \bar{N}^{21}_{\mathcal{H}} = \tfrac{1}{4}(-3+6r+15r^2) \\
& N^2_{\mathcal{H}2} = \tfrac{1}{2}(r^2-1) && \bar{N}^{22}_{\mathcal{H}} = \tfrac{1}{4}(-15+45r^2) \\
p=3 \quad & N^3_{\mathcal{H}0} = \tfrac{1}{2}(1-r) && \bar{N}^{30}_{\mathcal{H}} = \tfrac{1}{4}(-3+15r+15r^2-35r^3) \\
& N^3_{\mathcal{H}1} = \tfrac{1}{2}(1+r) && \bar{N}^{31}_{\mathcal{H}} = \tfrac{1}{4}(-3-15r+15r^2+35r^3) \\
& N^3_{\mathcal{H}2} = \tfrac{1}{2}(r^2-1) && \bar{N}^{32}_{\mathcal{H}} = \tfrac{1}{4}(-15+45r^2-15r^3) \\
& N^3_{\mathcal{H}3} = \tfrac{1}{2}(r^3-r) && \bar{N}^{33}_{\mathcal{H}} = \tfrac{1}{4}(-105r+175r^3),
\end{aligned}
\tag{87}
$$

with

$$
\delta^j_i = \int_{-1}^{+1} N^p_{\mathcal{H}_i}(r) \cdot \bar{N}^{pj}_{\mathcal{H}}(r) \mathrm{d}r. \tag{88}
$$

The topology matrix $\mathbf{T}$, see Eqs. (74), (80), is not regular and repeated as Eq. (A)

$$
\text{(A)} \qquad \mathbf{T} \cdot \hat{\bar{\mathbf{t}}}_h = \hat{\bar{\mathbf{p}}}_h(\mathbf{u}_h) \; ; \quad \det(\mathbf{T}^{\mathrm{T}}\mathbf{T}) = \mathbf{0}. \tag{89}
$$

In 2D problems there are one or more zero eigenvalues of $\mathbf{T}^{\mathrm{T}}\mathbf{T}$, and in 3D problems there are five or more zero eigenvalues.

The regularization of the local equation system for patch k is given by two additional conditions. The first *additional conditions* are posed on Neumann boundaries (with natural boundary conditions) where equilibrium with FE nodal forces is satisfied explicitly as

$$
\text{(B)} \qquad \hat{\bar{\mathbf{p}}}_h(\mathbf{t}) = \hat{\bar{\mathbf{t}}}_h \quad \text{on} \quad \Gamma_t. \tag{90}
$$

The second *additional condition* with FE stresses $\boldsymbol{\sigma}_h(\mathbf{u}_h)$ in Ω_e is gained by postulating that the boundary tractions from previous finite element solution $\mathbf{u}_h$ are approximately equal to the new tractions in the weak sense.

$$
\text{(C)} \qquad \int_{\partial\Omega_e} (\boldsymbol{\sigma}_h(\mathbf{u}_h) \cdot \mathbf{n})^{\mathrm{T}} \cdot \mathbf{v}_h \mathrm{d}O \simeq \int_{\partial\Omega_e} \mathbf{t}_h \cdot \mathbf{v}_h \mathrm{d}O \qquad \forall \mathbf{v}_h \in \mathbf{V}_h \,, \tag{91}
$$

$$
\underbrace{\int_{\partial\Omega_e} (\boldsymbol{\sigma}_h(\mathbf{u}_h) \cdot \mathbf{n})^{\mathrm{T}} \mathbf{N}_v \mathrm{d}O}_{\hat{\bar{\mathbf{p}}}_h(\boldsymbol{\sigma}_h)} \cdot \hat{\mathbf{v}}_h \simeq \hat{\bar{\mathbf{t}}}_h \int_{\partial\Omega_e} \frac{\underbrace{\bar{\mathbf{N}}^{\mathrm{T}}_t}_{\bar{\mathbf{N}}^{\mathrm{T}}_{\mathcal{L}}} \underbrace{\mathbf{N}_v}_{\mathbf{N}_{\mathcal{L}}} \mathrm{d}O \cdot \hat{\mathbf{v}}_h \,,}{\det(\boldsymbol{\mathcal{J}}(r,s))_{\partial\Omega_e}} \tag{92}
$$

$$
\hat{\bar{\mathbf{p}}}_h(\boldsymbol{\sigma}_h)^{\mathrm{T}} \hat{\mathbf{v}}_h \simeq \hat{\bar{\mathbf{t}}}_h \underbrace{\int_{\partial I} \frac{1}{\det(\boldsymbol{\mathcal{J}}(r,s))_{\partial\Omega_e}} \bar{\mathbf{N}}^{\mathrm{T}}_{\mathcal{L}} \mathbf{N}_{\mathcal{L}} \det(\boldsymbol{\mathcal{J}}(r,s))_{\partial\Omega_e} \mathrm{d}O}_{\mathbf{I}} \cdot \hat{\mathbf{v}}_h \tag{93}
$$

$$
\Rightarrow \quad \hat{\bar{\mathbf{p}}}_h(\boldsymbol{\sigma}_h) = \hat{\bar{\mathbf{t}}}_h \,. \tag{94}
$$

This results in a least square approximation

$$
\text{(C)} \qquad \frac{1}{2}(\hat{\bar{\mathbf{p}}}_h(\boldsymbol{\sigma}_h) - \hat{\bar{\mathbf{t}}}_h)^2 \to \min. \tag{95}
$$

Summarizing the calculation of tractions $\mathbf{t}$:

$$\left.\begin{array}{ll} \text{nodal forces} & \mathbf{T}\hat{\bar{\mathbf{t}}} - \hat{\bar{\mathbf{p}}}_h(\mathbf{u}_h) = \mathbf{0} \\ \text{boundary tractions} & \hat{\bar{\mathbf{t}}}_h - \hat{\bar{\mathbf{p}}}_h(\mathbf{t}) = \mathbf{0} \end{array}\right\} \quad \begin{array}{l} \text{exactly fulfilled} \\ \text{conditions (A), (B)} \end{array}$$

$$\text{regularization } \tfrac{1}{2}(\hat{\bar{\mathbf{p}}}_h(\boldsymbol{\sigma}_h) - \hat{\bar{\mathbf{t}}}_h)^2 \to \min \quad \begin{array}{l} \text{weakly fulfilled} \\ \text{conditions (C)} \end{array} \tag{96}$$

Remark: Further development are necessary to extend condition (C) to the weak form of field equations. To avoid locking effects the local approxiamtion space for stress calculation has to be expanded with further internal deformation modes, e.g. bubble modes.

6.1. Solution and model error estimation

After calculation of the equilibrated tractions the discretization error can be calculated by the difference between the equilibrated tractinos and the previous FE tractions with respect to the current stress approximation in the L_2- norm. For this, the local data of the current model with the approximation space $\mathbf{V}_h$ are:

$\hat{\mathbf{u}}_h$: local nodal displacement for each element in Ω_e; $\mathbf{u}_h = \mathbf{N}_v\hat{\mathbf{u}}_h$,

$\mathbf{K}_e$: local stiffness matrix for each element in Ω_e,

$\hat{\bar{\mathbf{p}}}_h = \mathbf{K}_e\hat{\mathbf{u}}_h$: local nodal forces for each element in Ω_e,

$\hat{\bar{\mathbf{p}}}_h(\boldsymbol{\sigma}_h\mathbf{n})$: local nodal boundary tractions, calculated with $\boldsymbol{\sigma}_h\mathbf{n}$; $\boldsymbol{\sigma}_h = \boldsymbol{\sigma}_h(\mathbf{u}_h)$,

$\mathbf{t}_h = \bar{\mathbf{N}}_t\hat{\bar{\mathbf{t}}}_h$: local boundary tractions, calculated with PEM,

$\hat{\bar{\mathbf{t}}}_h$: local nodal boundary tractions, calculated with PEM.

Introducing the local discretization error $\mathbf{e}_{h+} \in \mathbf{V}_{h+} \subset \mathbf{V}$ and the test spaces of the expanded and the current problem with $\mathbf{v}_+ \in \mathbf{V}_+ \in \mathbf{V}_{h+} \ominus \mathbf{V}_h \subset \mathbf{V}_{h+} \subset \mathbf{V}$, see Eq. (27), a local variational problem is formulated as

$$a(\mathbf{e}_{h+}, \mathbf{v}_+)\Omega_e = L(\mathbf{v}_+)_{\partial\Omega_e} \qquad \forall \mathbf{v}_+ \in \mathbf{V}_+; \mathbf{e}_{h+} \in \mathbf{V}_{h+} \tag{97}$$

with

$$\mathbf{V}_{h+} := \left\{\mathbf{v}_{h+} \in H_0^1(\Omega_e);\ \mathbf{v}_{h+} \text{ without rigid body modes}\right\} \tag{98}$$

and results in

$$L(\mathbf{v}_+)_{\partial\Omega_e} = \int_{\partial\Omega_e} \mathbf{v}_+^{\mathrm{T}}(\mathbf{t}_h - \boldsymbol{\sigma}_h(\mathbf{u}_h))\mathrm{d}O \tag{99}$$

with $\mathbf{t}_h$ is gained from PEM. Equation (97) represents the so-called main equation of error analysis, Eq. (27), without the residual term. Mechanically, Eq. (97) describe the weak equilibrium of the traction jumps between the improved the boundary tractions $\mathbf{t}_h$ and the boundary tractions $\boldsymbol{\sigma}_h(\mathbf{u}_h)\mathbf{n}$, and it yields $\mathbf{e}_{h+}$. Such the *discretization "equilibrium" error estimator* η_{De} in Ω_e results in

$$\eta_{De}^2 = a(\mathbf{e}_{h+}, \mathbf{e}_{h+})_{\Omega_e}\ ; \quad \mathbf{e}_{h+} \in \mathbf{V}_{h+}\,. \tag{100}$$

For model error estimation we introduce the local variational form for an hierarchically expanded model with the corresponding expanded discretized solution $\tilde{\mathbf{u}}_{h+}$

$$a_M(\tilde{\mathbf{u}}_{h+}, \mathbf{v}_{h+})_{\Omega_e} = L(\mathbf{v}_{h+})_{\partial\Omega_e}\ , \quad \forall \mathbf{v}_{h+} \in \mathbf{V}_{h+}; \tilde{\mathbf{u}}_{h+} \in \mathbf{V}_{h+} \tag{101}$$

with

$$L(\mathbf{v}_{h+})_{\partial\Omega_e} = \int_{\partial\Omega_e} \mathbf{v}_{h+}^{\mathrm{T}} \mathbf{t}_h \mathrm{d}O. \tag{102}$$

Equation (101) describes the weak equlibrium of the new boundary tractions $\mathbf{t}_h$ (of an element patch k) for the expanded model within element Ω_e. Then, the *"equilibrium" error estimator* η_{Me} in the energy norm within Ω_e is given by

$$\eta_{Me}^2 = a_M(\tilde{\mathbf{u}}_{h+} - \mathbf{u}_h, \tilde{\mathbf{u}}_{h+} - \mathbf{u}_h)_{\Omega_e} \; ; \quad \tilde{\mathbf{u}}_{h+} \in \mathbf{V}_{h+} \; ; \quad \mathbf{u}_h \in \mathbf{V}_h. \tag{103}$$

To avoid considerable influences of the discretization error onto the model error, the global discretization error has to be significantly smaller than the global model error, e.g. $\eta_M^2 \leq 10 \cdot \eta_D^2$. Remark: for model error estimation conditions of the reduced models and of the master model the following conditions are necessary:

- Both models have the same dimension for $\mathbf{u}_{h_{red}}$ and $\mathbf{u}_{h_{enh}}$,
- and the same dimension for $\boldsymbol{\varepsilon}_{h_{red}}$ and $\boldsymbol{\varepsilon}_{h_{enh}}$,
- as well as the same dimension for $\boldsymbol{\sigma}_{h_{red}}$ and $\boldsymbol{\sigma}_{h_{enh}}$.
- The boundaries and loadings have to be the same, i.e.

$$L(\mathbf{v}) = L_{red}(\mathbf{v}). \tag{104}$$

6.2. Different model error estimators

The model error estimator can be gained in different ways. In section 6.1 the model error estimator was calculated in the energy norm by using the error of the displacements, Eq. (103). This error leads to strong locking effects due to neglecting of the deformation modes in the reduced model. In this section we introduce different strategies for model error estimation. The model error of the reduced model with respect to the hierarchically expanded model is given by the variational problem Eqs. (101), (103) yielding $\tilde{\mathbf{u}}_{h+}$.

We are collecting the following possible model error estimators:
The estimator of the model displacement error derived from Eq. (103), is

$$\eta_{Mu_e}^2 = ||\tilde{\mathbf{u}}_{h+} - \mathbf{u}_h||_{E_M(\Omega_e)}^2. \tag{105}$$

Due to the discussed locking effects, this estimator is not reasonable. Next we introduce the model error estimator in the energy norm but using the stresses of the current and the expanded model. Herein, the locking phenomena do not appear because the reduced model (e.g. for a thin plate in bending) is introduced to get fairly accurate stresses without regarding deformation modes in thickness direction. This estimator reads

$$\eta_{M\boldsymbol{\sigma}_e}^2 = ||\tilde{\boldsymbol{\sigma}}_{h+} - \boldsymbol{\sigma}_h||_{E_M(\Omega_e)}^2. \tag{106}$$

A relative model error in the L_2-norm, taking into account the neglected deformation modes of the reduced model is given by

$$\zeta_{Mu_e}^2 = ||\tilde{\mathbf{u}}_{h+} - \mathbf{u}_h||_{L_2(\Omega_e)}^2 \tag{107}$$

which is useful for the expansion of 2D plate and shell model. For a pure displacement method an energy oriented estimator

$$\eta_{ME_e}^2 = ||\tilde{\mathbf{u}}_{h+}||_{E_M(\Omega_e)}^2 - ||\mathbf{u}_h||_{E(\Omega_e)}^2 \tag{108}$$

can be used, too. But in most investigated cases, this indicator tends to zero which is known from the good-minded convergence of the energy.
The next two examples show that the model-stress error in the energy norm $\eta_{M\boldsymbol{\sigma}_e}^2$ is a useful error estimator from the engineering point of view.

6.3. Simple example with one C1-element

This section illustrates the differences between the presented model error estimators. Two simple examples are given with one C1-element (trilinear isoparametric element) for linear elastic and nearly incompressible plane stress calculation (in $r-s-$parameter plane), using the reduced 2D model and for 3D elasticity with the enhanced model.

The first example has the geometry factor length/thickness = 1, see Fig. 6a, and the second one has the factor length/thickness = 10, see Fig. 6b. From the engineering point of view the relative model error has to be smaller in the second example.

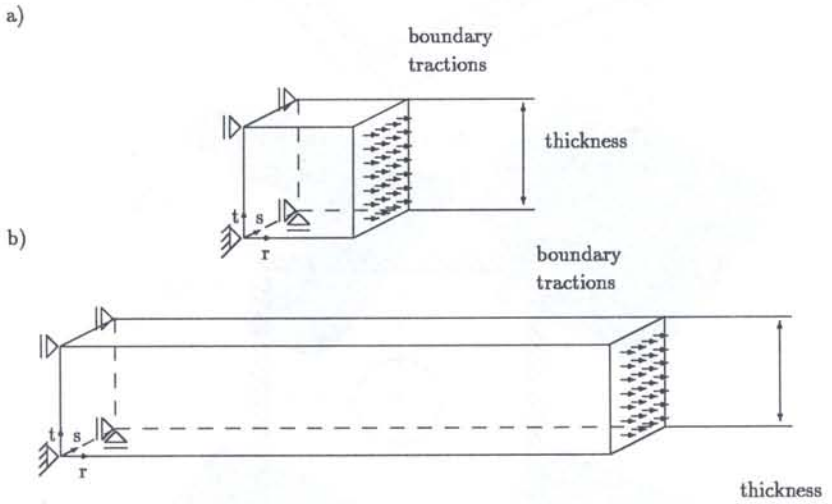

Fig. 6. Two simple examples for illustration the different model errors, a) short element, b) long element.

As already mentioned the error estimator η^2_{Mu} is not useful, see Tables 2 and 3. The error estimator $\eta^2_{M\sigma}$ yields reasonable results as well as the error estimator ζ^2_{Mu} in the L_2 norm, and they converge to zero if the element length tends to infinity.

Table 2. Model errors, Eqs. (105)–(108) for example 1, Fig. 6a

Error	$\nu = 0.0$	$\nu = 0.3$	$\nu = 0.499$
η^2_{Mu}	0%	12.1%	4160%
$\eta^2_{M\sigma}$	0%	0%	0%
ζ^2_{Mu}	0%	8.25%	19.8%
η^2_{ME}	0%	0%	0%

Table 3. Model errors, Eqs. (105)–(108) for example 2, Fig. 6b

Error	$\nu = 0.0$	$\nu = 0.3$	$\nu = 0.499$
η^2_{Mu}	0%	12.11%	4160%
$\eta^2_{M\sigma}$	0%	0%	0%
ζ^2_{Mu}	0%	0.09%	0.25%
η^2_{ME}	0%	0%	0%

6.4. Example: clamped thin plate in bending with a large hole

The plate is clamped at the edges and has constant transverse loading, see Fig. 7.

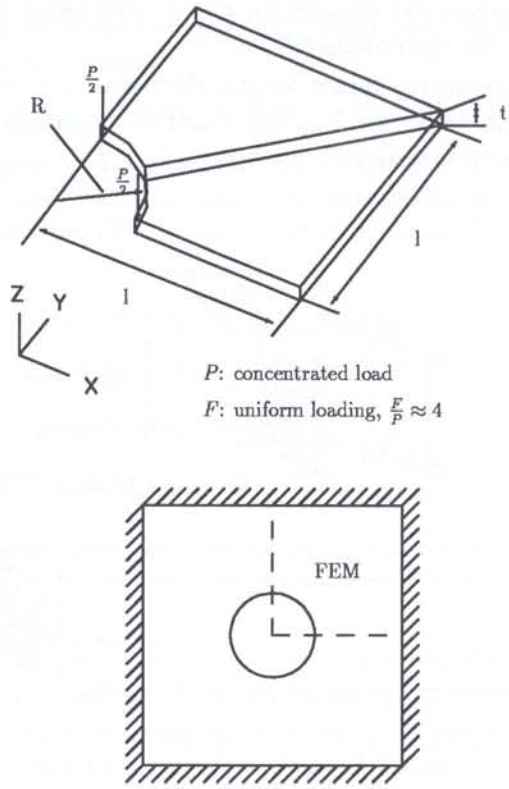

Fig. 7. System and system data of a clamped plate with a large hole with $l/t = 15$ and $l/R = 3$. In 2D Q2/P1 Reissner–Mindlin isoparametric elements with selective reduced integration are used, and in 3D C2 isoparametric elements are used.

Figure 8 shows a sequence of automatically adapted meshes for solution, dimension and model adaptivity within the expansion strategy. The lights regions are calculated with the 2D model and the dark regions are calculated with the 3D model. The model stress error estimator, Eq. (106), was used. This example shows that the model error estimator cover regions which are disturbed with respect to the master model. Near the system boundaries and near the concentrated loads at the hole boundary the model adaptivity takes place.

7. Conclusions

A new generation of adaptive numerical methods in structural mechanics was outlined, namely the full integration of solution, dimensional and model errors into well known h–p-adaptive concepts for boundary value problems of stiffened plates and shells.

The resulting anisotropic error indicators admit optional h- and p-adaptive processes but moreover d-adaptivity for plates and shells, i.e. dimensional expansions of the approximation space and even the update of the mathematical model, i.e of constitutive and geometrical equations. It is evident from the effectivity index that the expansion method — developing from lower to higher approximation spaces and also from reasonably simple to more complicated mathematical models in disturbed subdomains — is more efficient than the reduction method, which starts with the

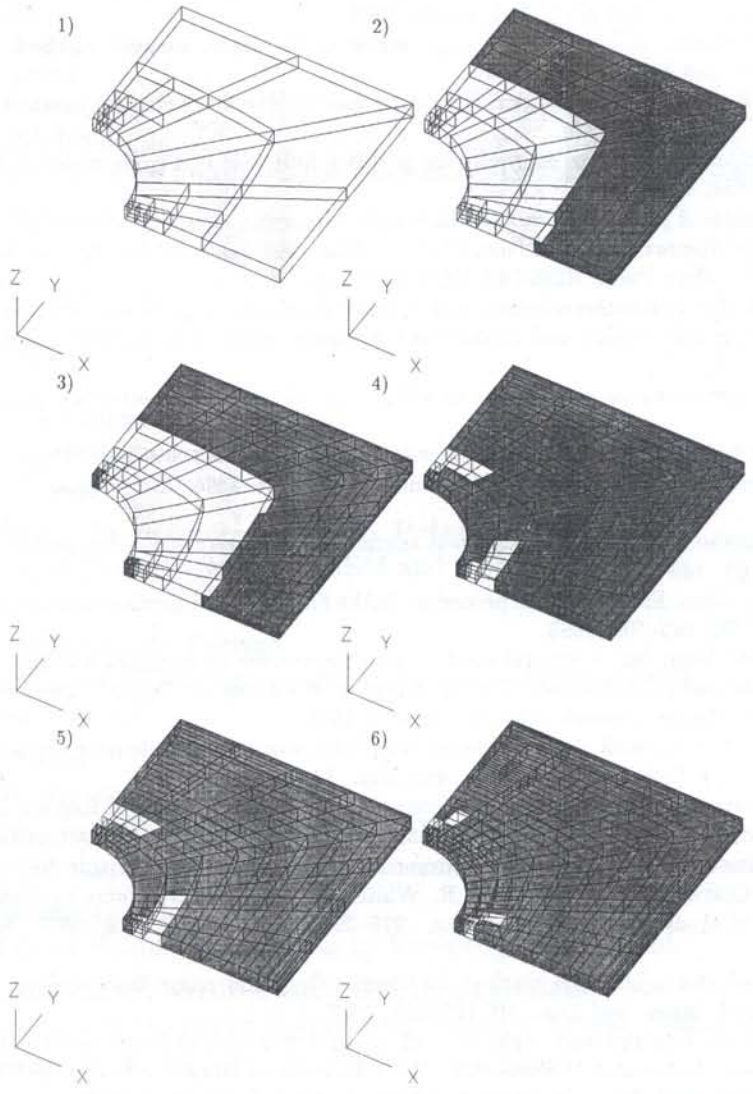

Fig. 8. Automatically refined meshes due to solution, dimension and model adaptivity; the light regions are calculated with the 2D model and the dark regions with the 3D model.

highest model and searches for simpler models in subdomains, e.g. by means of kinematic hypothesis. This holds especially for complicated stiffened thin-walled structures. And last but not least this expansion method corresponds to the typical engineering way of thinking.

Residual error estimators on patches with enhanced anisotropic test spaces are beneficial for solution and dimension adaptivity. Residual error estimators are insufficient for model adaptivity because the residual model error becomes very large (due to wrong stresses in enhanced model).

The Posteriori Equlibrium Method (PEM) yields physically consistent orthogonalized boundary tractions $\mathbf{t}_h$ for the expanded model, and it provides us with solution- and model-error estimators form local variational problems on patches which can be interpreted as a regularized Trefftz–method on element patches boundaries.

The mathematical analysis is still in progress, and further developments of PEM and related error estimators, including more complex material behaviour like plasticity or deformations of reinforced concrete in state 2 are scheduled.

REFERENCES

[1] M. Ainsworth, J.T. Oden. A procedure for a posteriori error estimation for $h-p$ finite element methods. *Comp.Meth. in Appl.Mech. and Eng.*, **101**: 73–96, 1992.

[2] I. Babuška. Some aspects of the h and $h-p$ version of the finite element method. *Numerical Methods in Engineering Theory and Applications*, 1987.

[3] I. Babuška, W.C. Rheinholdt. A–posteriori error estimates for the finite element method. *Int. Journal for Num. Meth. in Eng.*, **12**: 1597–1615, 1978.

[4] I. Babuška, W.C. Rheinholdt. Error estimates for adaptive finite element computations. *SIAM Journal on Num. Analysis*, **15**: 736–754, 1978.

[5] I. Babuška, C. Schwab. *A posteriori error estimation for hierarchic models of elliptic boundary value problems on thin domains.* Techn. Report, Technical Note BN 1148, May 1993, Institute for Physical Sciences and Technology, Univ. of Maryland College Park, MD20740, USA, 1993.

[6] H. Bufler, E. Stein. Zur Plattenberechnung mittels finite Elemente. *Ing. Archiv*, **39**: 248–260, 1970.

[7] W. Hackbusch. *Multi-grid method and applications.* Springer Series in Computational Mathematics, Springer–Verlag, Berlin, **4**, 1985.

[8] W. Hackbusch. *Integralgleichungen, Theorie und Numerik.* Teubner Studienbücher, Mathematik, ISBN 3–519–02370–9, 1989.

[9] S. Jensen. *Adaptive dimensional reduction for scalar boundary value problems.* Department of Mathematics, University of Maryland Baltimore Country, Baltimore, MD 21228–5398 USA, January 7,1991, revised November 8, 1991.

[10] C. Johnson, P. Hansbo. Adaptive finite element methods in computational mechanics. *Comp. Meth. in Appl. Mech. and Eng.*, **101**: 143–181, 1992.

[11] P. Ladevèze, D. Leguillon. Error estimate procedure in the finite element method and applications. *SIAM Journal on Num. Analysis*, **20**: 485–509, 1983.

[12] P. Ladevèze, E.A.W. Maunder. A general methodology for recovering equilibration finite element tractions and stress fields for plate and solid elements. *The First Intern. Workshop on Trefftz Method recent developments and perspectives*, 34–35, Cracow, Poland, May 30 – June 1, 1995.

[13] J.T. Oden, W.Wu, M. Ainsworth. An a posteriori error estimator for finite element approximation of the Navier–Stokes equation. *Comp. Meth. in Appl. Mech. and Eng.*, **111**: 185–202, 1994.

[14] C. Schwab. *A posteriori error estimation for hierarchic plate models.* Technical Report, Institute for Supercomputing and Applied Mathemathics, University of Maryland, IBM Scientific Centre, Heidelberg.

[15] E. Stein. The practical treatment of stress concentration and singularities within finite element displacement algorithms. In: P. Grisvard, W. Wendland, J.R. Whiteman, eds., *Lecture Notes in Mathematics, Singularities and Constructive Methods for Their Treatment*, 278–299. Proc. Oberwolfach 1983, Springer–Verlag Berlin, 1983.

[16] E. Stein, R. Ahmad. An equlibrium method for stress calculation using finite element displacement models. *Comp. Meth. in Appl. Mech. and Eng.*, **10**: 175–198, 1977.

[17] E. Stein, S. Ohnimus. Concept and realisation of integrated adaptive finite element methods in solid– and structural–mechanics. *Numerical Methods '92*, 163–170. Proc. of the First European Conf. on Num. Meth. in Eng., 7–11 September 1992. Brussels, Belgium, Elsevier Science Publ. B.V., 1992.

[18] E. Stein, S. Ohnimus. Expansion method for the integrated solution– and model–adaptivity within the FE–analysis of plates and shells. In: *Advances in finite element technology*, Ed. N.-E. Wiberg, CINME — Handbooks, Barcelona, Spain, 1995.

[19] E. Stein, S. Ohnimus. Dimensional adaptivity in linear elasticity with hierarchical test–spaces for $h-$ and $p-$refinement processes. *Engineering with Computers*, **12**: 107–119, 1996.

[20] E. Stein, W. Rust, S. Ohnimus. $h-$ and $d-$adaptive FE element methods for two–dimensional structural problems including postbuckling of shells. *2nd Reliability Colloqium*, Cracow,1991, *Comp. Meth. in Appl. Mech. and Eng.*, **101**: 315–354, 1992.

[21] E. Stein, B. Seifert, S. Ohnimus, C. Carstensen. Adaptive finite element analysis of geometrically non–linear plates and shells, especially buckling. *Int. Journal for Num. Meth. in Eng.*, **37**:2631–2655, 1994.

[22] W. Wunderlich, G. Kiener, W. Osterman. Modellierung und Berechnung von Deckenplatten mit Unterzügen. *Bauingenieur* **69**: 381–390, 1994.

[23] O.C. Zienkiewicz, J.Z. Zhu. A simple error estimator and adaptive procedure for practical engineering analysis. *Int. Journal for Num. Meth. in Eng.*, **24**: 337–357, 1987.

[24] O.C. Zienkiewicz, J.Z. Zhu. The superconvergent patch recovery and a posteriori error estimators, part 1: The recovery technique. *Int. Journal for Num. Meth. in Eng.*, **33**: 1333–1364, 1992.

[25] O.C. Zienkiewicz, J.Z. Zhu. The superconvergent patch recovery and a posteriori error estimators, part 2: Error estimators and adaptivity. *Int. Journal for Num. Meth. in Eng.*, **33**: 1365–1382, 1992.